NISTIR 6937

ENERGY DISSIPATION DEVICES FOR BRIDGES WITH STEEL SUPERSTRUCTURES

Michael A. Riley

Building and Fire Research Laboratory
Gaithersburg, MD 20899-8611

United States Department of Commerce
Technology Administration
National Institute of Standards and Technology

NISTIR 6937

ENERGY DISSIPATION DEVICES FOR BRIDGES WITH STEEL SUPERSTRUCTURES

Michael A. Riley

April 2003

Building and Fire Research Laboratory
National Institute of Standards and Technology
Gaithersburg, MD 20899-8611

United States Department of Commerce
Donald L. Evans, *Secretary*

Technology Administration
Phillip J. Bond, *Under Secretary for Technology*

National Institute of Standards and Technology
Arden L. Bement, Jr., *Director*

ABSTRACT

Recent earthquakes have clearly demonstrated the seismic vulnerability of bridges constructed with steel superstructures. The relative flexibility of these bridges, especially in the transverse direction, may result in overstressing or even failure of components, including trusses, end diaphragms, beams, bearings, piers, and columns. For the case of slab-on-girder steel bridges, flexible end diaphragms may experience large deformations, leading to buckling or brittle fracture during seismic excitations. However, if the end diaphragms are too stiff, the forces transmitted through the diaphragms to the bearings and substructure may lead to damage or failure in the supporting system. Structural dampers and other energy dissipation techniques are viable options to enhance the ductility and energy dissipation capacity of the diaphragms, thereby increasing the safety and reliability of the bridges. Prior research has clearly shown that ductile end diaphragms can greatly improve the response of steel slab-on-girder bridges; however, only a limited number of the many available energy dissipation devices have been investigated. This research effort has focused on analyzing the response of steel slab-on-girder bridges that incorporate a wide variety of passive energy dissipation devices in a number of different configurations. The results of this work show what devices and bracing configurations can best improve the response of slab-on-girder bridges to strong seismic loads.

ACKNOWLEDGEMENTS

This research was supported by a grant from the Multidisciplinary Center for Earthquake Engineering Research (MCEER) through the MCEER Highway Project, which was funded by the Federal Highway Administration (FHWA) through contract DTFH61-98-C-00094. The support of MCEER and the FHWA is gratefully appreciated.

CONTENTS

Abstract iii

Acknowledgements v

Contents vii

List of Figures ix

1 Introduction 1

1.1 Previous Research 1
1.2 Objective of Current Research 2

2 Bridge Models 3

2.1 Scale Model Bridge 3
2.2 Numerical Model 4

3 Control Devices and Configurations 7

3.1 Control Devices Considered 7
3.1.1 Yielding Metallic Devices 7
3.1.2 Friction Devices 7
3.1.3 Fluid Viscous Devices 8
3.1.4 Viscoelastic Devices 8
3.2 Control Device Configurations 9

4 Response of Scaled Model Bridge 11

4.1 Response with Viscous Fluid Dampers 11
4.2 Response with Friction Dampers 19
4.3 Response with Viscoelastic Dampers 26
4.4 Response with TADAS Elements 32

5 Conclusions 37

6 References 39

LIST OF FIGURES

Figure 2.1. Full scale bridge model elevation. 3
Figure 2.2 Full scale bridge model – transverse bracing at abutments. 4
Figure 2.3 Full scale bridge model –general transverse bracing. 4
Figure 2.4. 2/5 Scale bridge model – transverse bracing at abutments. 5
Figure 2.5. 2/5 Scale bridge model – general transverse bracing. 5
Figure 2.6. Three dimensional view of numerical model. 6
Figure 3.1 Force displacement loops for friction devices. 7
Figure 3.2 Force-displacement loops for fluid viscous devices. 8
Figure 3.3 Force-displacement loops for viscoelastic devices. 9
Figure 3.4. Configuration with dampers inserted into existing cross-braces. 10
Figure 3.5. Configuration with dampers inserted into chevron cross-braces. 10
Figure 4.1 Deck displacement ratio with viscous fluid dampers in cross braces. 11
Figure 4.2 Shear Connector stress ratio with viscous fluid dampers in cross braces. 12
Figure 4.3 Peak forces in viscous fluid dampers in cross braces. 13
Figure 4.4 Base shear ratio with viscous fluid dampers in cross braces. 13
Figure 4.5 Deck displacement ratio with viscous fluid dampers in chevron braces. 14
Figure 4.6 Shear connector stress ratio with viscous fluid dampers in chevron braces. 15
Figure 4.7 Peak forces in viscous fluid dampers in chevron braces. 16
Figure 4.8 Base shear ratio with viscous fluid dampers in chevron braces. 16
Figure 4.9 Deck displacement ratio with viscous fluid dampers connected to abutments. 17
Figure 4.10 Shear connector stress ratio with VF dampers connected to abutments. 17
Figure 4.11 Peak forces in viscous fluid dampers connected to abutments. 18
Figure 4.12 Base shear ratio with viscous fluid dampers connected to abutments. 18
Figure 4.13 Deck displacement ratio with friction dampers in cross braces. 20
Figure 4.14 Shear connector stress ratio with friction dampers in cross braces. 20
Figure 4.15 Peak forces in friction dampers in cross braces. 21
Figure 4.16 Base shear ratio with friction dampers in cross braces. 21
Figure 4.17 Deck displacement ratio with friction dampers in chevron braces. 22
Figure 4.18 Shear connector stress ratio with friction dampers in chevron braces. 22
Figure 4.19 Peak forces in friction dampers in chevron braces. 23
Figure 4.20 Base shear ratio with friction dampers in chevron braces. 23
Figure 4.21 Deck displacement ratio with friction dampers connected to abutments. 24
Figure 4.22 Shear connector stress ratio with friction dampers connected to abutments. 24
Figure 4.23 Peak forces in friction dampers connected to abutments. 25
Figure 4.24 Base shear ratio with friction dampers connected to abutments. 25
Figure 4.25 Deck displacement ratio with VE dampers in chevron braces. 26
Figure 4.26 Shear connector stress ratio with VE dampers in chevron braces. 27
Figure 4.27 Base shear ratio with VE dampers in chevron braces. 27
Figure 4.28 Peak damping forces in VE dampers in chevron braces. 28
Figure 4.29 Peak stiffness forces in VE dampers in chevron braces. 28
Figure 4.30 Deck displacement ratio with VE dampers connected to abutments. 29
Figure 4.31 Shear connector stress ratio with VE dampers connected to abutments. 30
Figure 4.32 Base shear ratio with VE dampers connected to abutments. 30
Figure 4.33 Peak damping forces in VE dampers connected to abutments. 31
Figure 4.34 Peak stiffness forces in VE dampers connected to abutments. 31

Figure 4.35 Deck displacement ratio with TADAS elements in chevron braces. 33
Figure 4.36 Shear connector stress ratio with TADAS elements in chevron braces. 33
Figure 4.37 Base shear ratio with TADAS elements in chevron braces. 34
Figure 4.38 Peak forces in TADAS elements in chevron braces. 34
Figure 4.39 Deck displacement ratio with TADAS elements connected to abutments. 35
Figure 4.40 Shear connector stress ratio with TADAS elements connected to abutments. 35
Figure 4.41 Base shear ratio with TADAS elements connected to abutments. 36
Figure 4.42 Peak forces in TADAS elements connected to abutments. 36

1 INTRODUCTION

Recent earthquakes have clearly demonstrated the seismic vulnerability of bridges constructed with steel superstructures (Housner and Thiel, 1995; Astaneh-Asl et al., 1994). The relative flexibility of these bridges, especially in the transverse direction, may result in overstressing or even failure of components; including trusses, end-diaphragms, beams, bearings, piers, and columns. For the case of slab-on-girder steel bridges, flexible end diaphragms may experience large deformations leading to buckling or brittle fracture during seismic excitations. However, if the end diaphragms are too stiff, the forces transmitted through the diaphragms to the bearings and substructure may lead to damage or failure in the supporting system.

Seismic isolation is often an effective method of protecting such bridges from strong earthquakes. Unfortunately, in many cases the cost of retrofitting existing bridges this way can be quite high, due to the need for abutment and pier modifications to allow for the large superstructure deflections associated with the isolation devices.

Innovative techniques such as passive energy dissipation and semi-active devices are viable alternative options that enhance the ductility and energy dissipation capacity of the diaphragms, thereby increasing the safety and reliability of steel bridges. Such devices can be retrofitted into existing steel bridges, or used in new bridges, either with or without seismic isolation.

1.1 Previous Research

Passive energy dissipation devices, commonly known as structural dampers, have been used in various forms for more than a quarter of a century. They have mostly been used to increase the damping of frame buildings subjected to earthquakes or strong winds, or to provide additional damping in seismic isolation systems for building or bridges. Extensive information on the development of these devices, theory of their operation, and methods for designing structures that incorporate them can be found in, among other sources, Soong and Dargush (1997), Hanson and Soong (2001).

The use of passive energy dissipation devices to improve the response of slab-on-girder highway bridges has only been considered recently. In the aftermath of the Northridge and Kobe earthquakes, efforts were undertaken to quantify the effects of the diaphragms on the seismic response of these bridges (Zahrai and Bruneau, 1998). This work showed that only the end diaphragms played a significant role in the lateral response of the bridge. In addition, this research showed that only a small amount of stiffness in the end diaphragms was necessary to cause the girders and deck to act as a rigid unit, while the diaphragms were intact. However, once the diaphragms failed large lateral deformations could occur in the girders, leading to severe damage.

This finding led to the proposal to use in the diaphragms and bracing of steel deck-truss and slab-on-girder bridges ductile members that employ either yielding metallic dampers or sacrificial shear panels (Sarraf and Bruneau, 1998a, 1998b; Zahrai and Bruneau, 1999a; 1999b). These authors showed that such energy dissipation techniques could be successfully retrofitted into existing highway bridges that do not meet current seismic requirements. Additional research (Zahrai and Bruneau, 1999b) included experimental testing of three types of ductile end diaphragms for a slab-on-girder bridge.

Tests were performed on specimens fitted with diaphragms that utilized eccentrically braced frames, sacrificial shear panels, and triangular-plate added damping and stiffness (TADAS) devices. The results of the tests showed that each of these diaphragm designs could provide the stiffness and energy dissipation necessary for a retrofitted bridge to withstand moderate to large earthquakes.

1.2 Objective of Current Research

The work described above has clearly shown that ductile end diaphragms can greatly improve the response of steel slab-on-girder bridges. However, that work has only scratched the surface with regard to the available methods of providing energy dissipation, as it has examined only a limited number of the many possible energy dissipation devices that are available.

The research effort reported in this work is focused on analyzing the response of steel slab-on-girder bridges that incorporate a wider variety of passive energy dissipation devices in a number of different configurations. The objective of this work is to determine which devices and configurations can best improve the response of these bridges to extreme seismic loads.

2 BRIDGE MODELS

All of the bridge models used in this study were based on the bridge configuration used by Buckle and Itani in the University of Nevada, Reno (UNR) study. This bridge model was, in turn, based on a typical CALTRANS slab-on-girder highway bridge.

The model bridge, shown in Figure 2.1 through Figure 2.3, is a three- lane bridge with four 1.52 m (5 ft) deep girders spaced 3.35 m (11 ft) on center. The girders are constructed of A709 Gr50 steel plate, with 22.2 mm (7/8 in) thick plates used for the webs and 44.5 mm (1 ¾ in) thick by 457 mm (18 in) wide plates used for the flanges. The reinforced concrete deck slab is 12.95 m (42 ft 6 in) wide by 219 mm (8 5/8 in) thick. The deck was further thickened through a series of haunches to a depth of 305 mm (12 in) above the girders. The concrete in the deck has an f_c' of 27.6 MPa (4 ksi).

In the design configuration, the bridge was laterally braced with cross frames consisting of single 101.6 mm x 101.6 mm x 15.9 mm (4 in x 4 in x 5/8 in) angles, as shown in Figure 2.2. These cross-frames were attached to 19.1 mm (3/4 in) thick web stiffeners. To transfer the lateral loads to the cross-frames equally, 101.6 mm x 101.6 mm x 15.9 mm (4 in x 4 in x 5/8 in) double angle struts were used to connect the tops and bottoms of the web stiffeners. An exception was made at the abutment ends of the bridge, where 267 mm x 452 N/m (WT10.5 x 31) top struts were used in place of the double angles; these struts were not used to provide additional lateral stiffness, but instead to transfer impact loads, caused by traffic passing onto the bridge, more directly from the deck to the girders.

In its design configuration, the bridge had four spans supported on abutments at either end and on three 9.75 m (32 ft) high piers. The end spans were each 40.4 m (132 ft 6 in) long, while the center spans were each at 48.8 m (160 ft) long. The piers were single column bents with 1.83 m (6 ft) diameter columns and 2.13 m (7 ft) wide by 1.83 m (6 ft) high pier caps. The lateral braces were located at the abutments and piers, and at 4.57 m (15 ft) and 10.7 m (35 ft) on either side of the piers and abutments.

2.1 Scale Model Bridge

The primary model used for numerical simulations was based on the 2/5-scale model bridge used for experimental testing at the University of Reno-Nevada. This bridge model is a single span, two girder scaled version of the full-scale model, as shown in Figures 2.4 and 2.5.

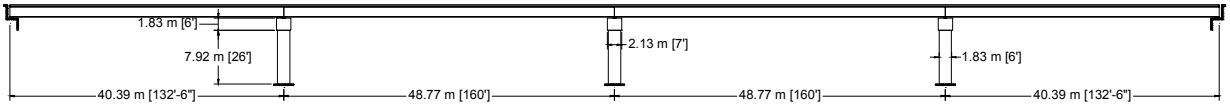

Figure 2.1 Full scale bridge model elevation.

The scale model is 18.3 m (60 ft) long, with two 610 mm (2 ft) deep girders. The girders are constructed with 9.53 mm (3/8 in) thick plates used for the webs and 19.1 mm (3/4 in) thick by 184 mm (7.25 in) wide plates used for the flanges. The girders are centered 1.34 m (4 ft 4 ¾ in) apart laterally. The reinforced concrete deck is 2.50 m (8 ft 2 ½ in) wide and 88.9 mm (3 ½ in) thick.

The bridge is laterally braced every 3.05 m (10 ft) with cross frames consisting of a single 50.8 mm x 50.8 mm x 6.35 mm (2 in x 2 in x 1/4 in) angles, with 50.8 mm x 50.8 mm x 6.35 mm (2 in x 2 in x 1/4 in) double angles providing additional lateral stiffness at the tops and bottoms of the lateral diaphragms. These struts were connected to 9.53 mm (3/8 in) thick web stiffeners. In a similar manner to the full-scale bridge, for the end frames 102 mm x 73 N/m (WT4 x 5) top struts were used in place of the double angles.

2.2 Numerical Model

A numerical model of the bridge was developed using the computer program "SAP2000 Nonlinear". The deck of the bridge was modeled using thick shell elements and the main beams were modeled with thin shell elements, which allowed the local stresses in the steel sections to be considered. Short shear elements were used to model the shear keys in the bridge and allow for the composite action between the deck and the beams. The braces in the diaphragms were modeled with frame elements, while the isolators and control devices were modeled using the appropriate

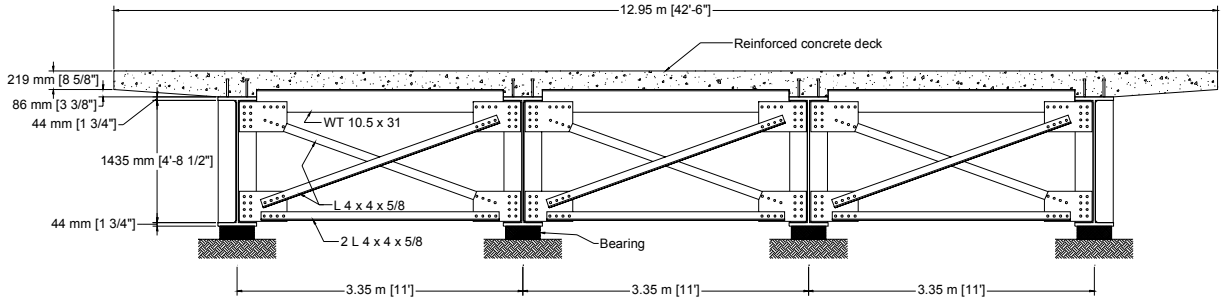

Figure 2.2 Full scale bridge model – transverse bracing at abutments.

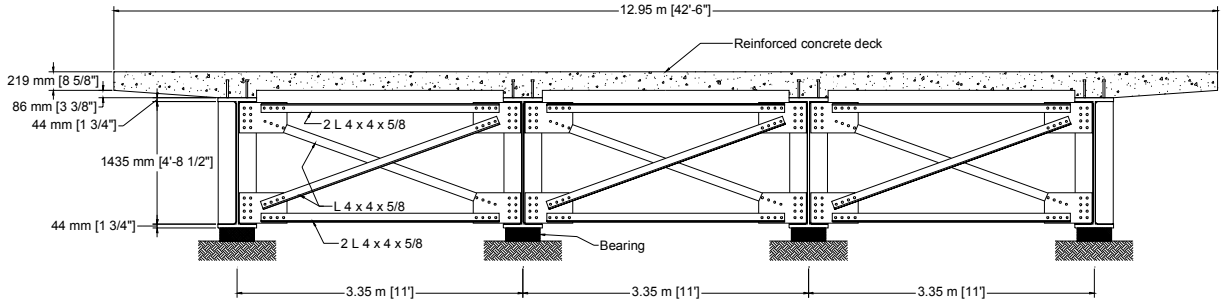

Figure 2.3 Full scale bridge model –general transverse bracing.

nonlinear elements. An image of the model showing the shell elements and joints can be seen in Figure 2.6.

The size of the shell elements were chosen so that their shape factors were reasonable and would not adversely impact the simulations, but they were made as large as reasonable to minimize the required computation time.

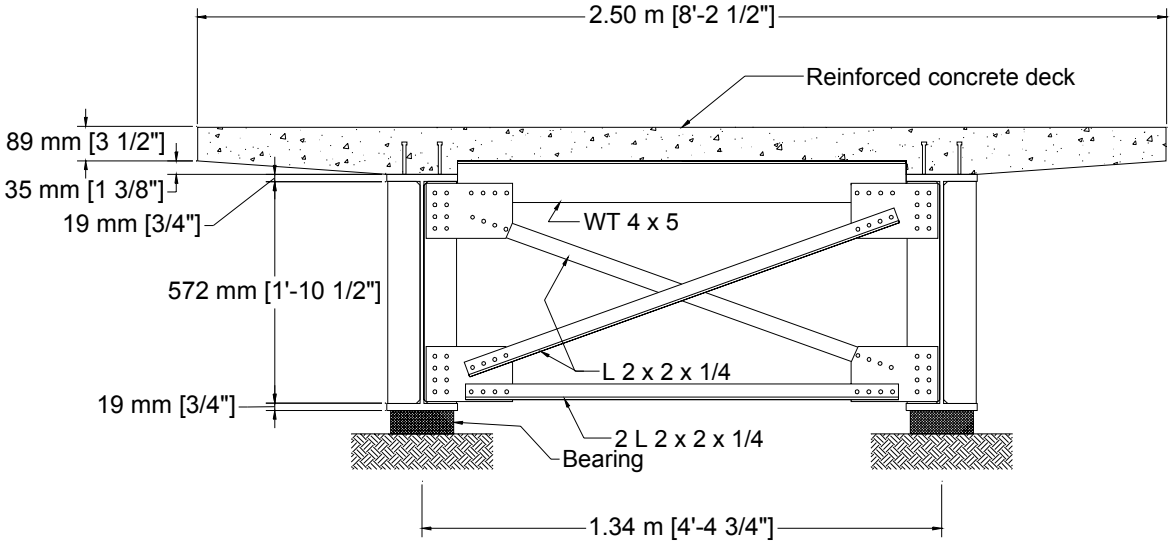

Figure 2.4 2/5 Scale bridge model – transverse bracing at abutments.

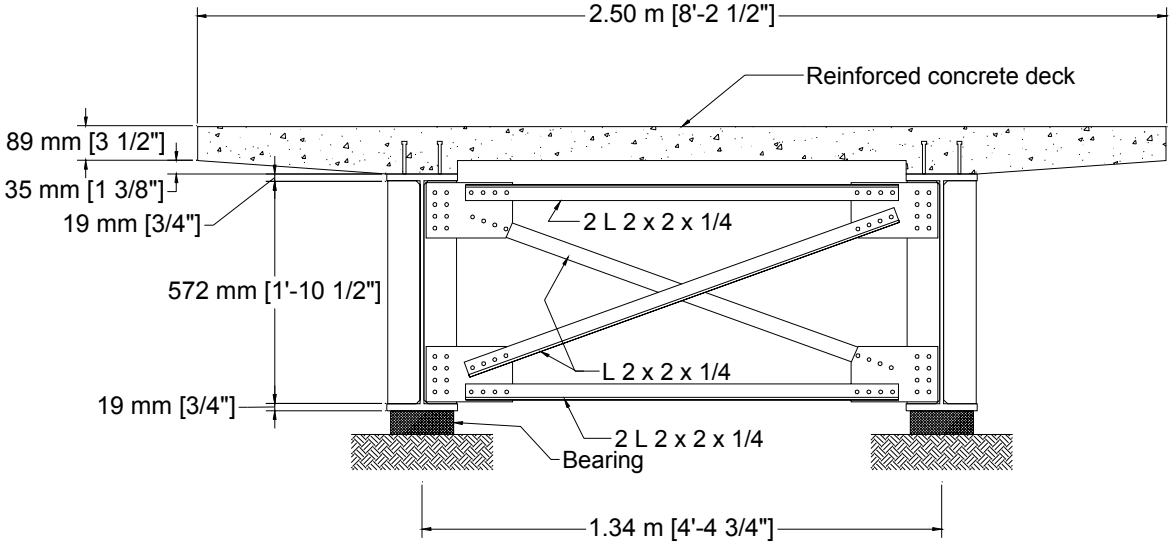

Figure 2.5 2/5 Scale bridge model – general transverse bracing.

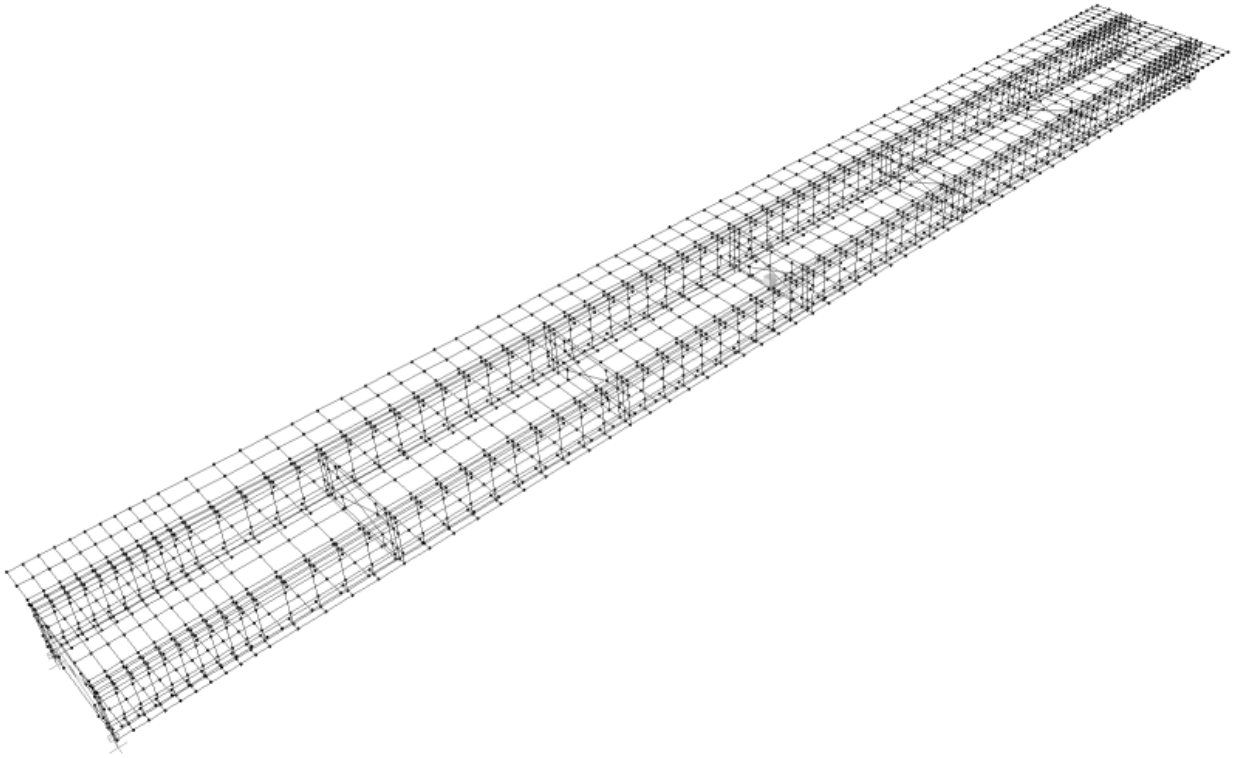

Figure 2.6 Three dimensional view of numerical model.

3 CONTROL DEVICES AND CONFIGURATIONS

Four types of structural dampers were considered in this investigation. Yielding plate dampers (TADAS) elements were used in a configuration similar to that used by Zahrai and Bruneau (1999b). In addition, these devices were used in a configuration where devices were connected between the tops of the bridge beams and the bridge piers or abutments. Sliding friction dampers, viscoelastic dampers, and viscous fluid dampers were all used to replace the diagonal braces in the end frames of the bridge, and to connect the tops of the beams to the bridge piers or abutments.

Details of the devices and brace configurations that were used follow.

3.1 Control Devices Considered

3.1.1 Yielding Metallic Devices

Metallic yielding devices take advantage of the stable hysteretic force-displacement behavior of metals to absorb energy in structures. These devices have taken many forms, which use flexural, shear, or extensional deformations in the plastic range to provide the structure with increased stiffness and energy dissipation capacity. Yielding devices have most often been used in the bracing systems of building frames or to provide additional damping for seismic isolators for both buildings and bridges.

In this work, triangular added damping and stiffness (TADAS) devices were chosen. These devices consist of a number of thin triangular plates, with their bases rigidly anchored and their tips connected to a strut such that they are deformed in bending by the deflections of the structure. The individual plates are designed so that they will yield over their entire length when the yield stress is reached. Thus these devices exhibit linear stiffness until they yield, after which they exhibit a force-displacement behavior that can be approximated by a bilinear model.

Their response can be characterized by the size and number of the triangular plates, and by the material properties, as described in the work of Tsai, et al (1993).

3.1.2 Friction Devices

Friction devices employ the friction forces between metal surfaces. These forces can be modeled as simple Coulomb friction, so the force-displacement curves of the device, as shown in Figure 3.1, are rectangular hysteresis loops. The damping mechanism can be a friction joint located at the intersection of cross braces in frames; a device that is attached to the bracing system and utilizes friction between metal surfaces, friction pads, or wedges; or a device that allows slip to take place in slotted connections. The devices can be characterized by their slip-displacement and slip-load.

For design purposes, the slip-load can be

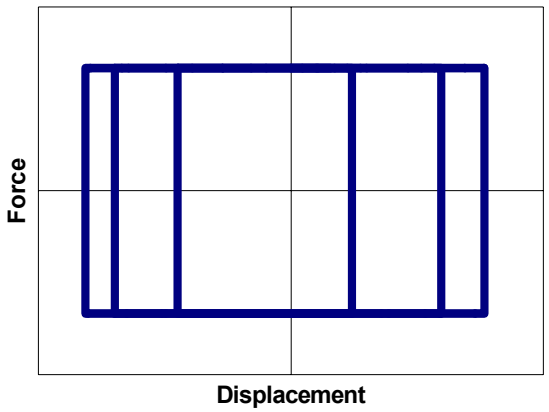

Figure 3.1 Force displacement loops for friction devices.

chosen based on the expected forces and displacements in the structure. By adjusting the clamping force on the sliding surfaces of the device a wide range of slip forces can be achieved. The slip displacement can be controlled by adjusting the stiffness of the mounting braces. The energy dissipated by the device during one cycle of motion, E_D, is equal to the area of the force displacement curve. The energy that will be dissipated during a design event, for which the design displacement of the devices are known, can be set by adjusting the slip force.

3.1.3 Fluid Viscous Devices

Fluid viscous devices are used in a variety of structures and mechanical systems to reduce vibrations and impact loads. The devices are typically attached to the bracing system in buildings. They utilize the dissipation that occurs in fluid flow through orifices, and their cyclic response is a function of the relative velocity between the ends of the damper. The devices generally generate only damping forces, but they may exhibit some stiffness at high frequencies.

For the case of a linear device that does not exhibit stiffness in the high frequency range,

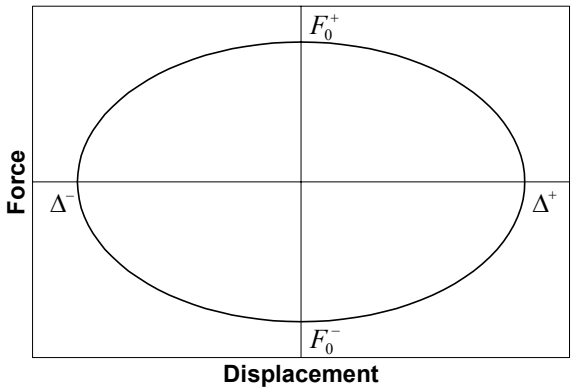

Figure 3.2 Force-displacement loops for fluid viscous devices.

the damping force can be expressed as simply:

$$F = C\dot{\Delta} \tag{3.1}$$

where C is the damping coefficient and $\dot{\Delta}$ is the stroke velocity. The curve formed by this idealized force-displacement response is shown in Figure 3.2. These devices can be designed to have a wide variety of damping coefficients and stroke lengths.

3.1.4 Viscoelastic Devices

Viscoelastic damping devices are constructed from constrained layers of acrylic polymers. They are designed so that relative motion between the ends of the device is translated into shear deformation in the polymer layers. When deformed, the viscoelastic materials exhibit combined features of elastic solid and viscous liquid. These devices commonly are used in the bracing system of moment resisting frames as energy dissipators for wind and seismic excitations.

The devices can be modeled as a spring and dashpot in parallel (Kelvin model), with the force expressed by:

$$F = K_{eff}\Delta + C\dot{\Delta} \tag{3.2}$$

Here, Δ and $\dot{\Delta}$ are the stroke and stroke velocity of the device, *C* is the damping coefficient, and K_{eff} is the effective stiffness of the device. The effective stiffness of a device can be computed as:

$$K_{eff} = \frac{F^+ - F^-}{\Delta^+ - \Delta^-} \tag{3.3}$$

Here, F^+ and F^- are the forces corresponding to the maximum and minimum displacements, Δ^+ and Δ^-, respectively, as

indicated in Figure 3.3. The damping coefficient of the device can then be expressed as:

$$C = \frac{E_D}{\pi \omega \Delta_{ave}^2} \tag{3.4}$$

Here, E_D is the dissipated energy, which is equal to the area enclosed by one complete cycle of the force-displacement response, ω is the angular frequency, and Δ_{ave} is the average of the magnitudes of Δ^+ and Δ^-. The effective stiffness and the damping coefficient of a viscoelastic device are generally dependent on the excitation frequency and the operating temperature, including the temperature rise due to excitation.

3.2 Control Device Configurations

Three device configurations were used in this study. The first configuration, shown in Figure 3.4, used devices inserted into the existing cross braces of the end diaphragms. This configuration is practical for many types of structural dampers, but not for all. In particular, the TADAS dampers cannot be easily used in this configuration.

The second configuration, shown in Figure 3.5, used chevron braces with the damper located between the diagonal braces and the bottom strut of the diaphragm. This is the configuration used with the TADAS elements and ductile shear panels in previous research (Zahrai and Bruneau, 1999b).

The third configuration was similar to the previous one, except that a strut was used to connect the damping element directly to the bridge abutment, instead of the bottom strut of the diaphragm. This configuration has the advantage of including both lateral the deformations in the end diaphragm and the deformations in the bridge bearings in the motion that activates the damper.

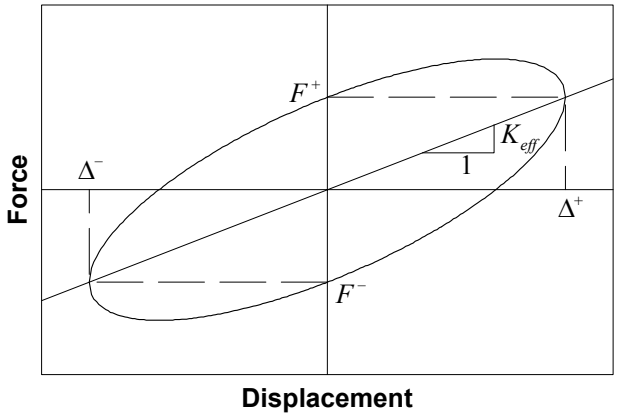

Figure 3.3 Force-displacement loops for viscoelastic devices.

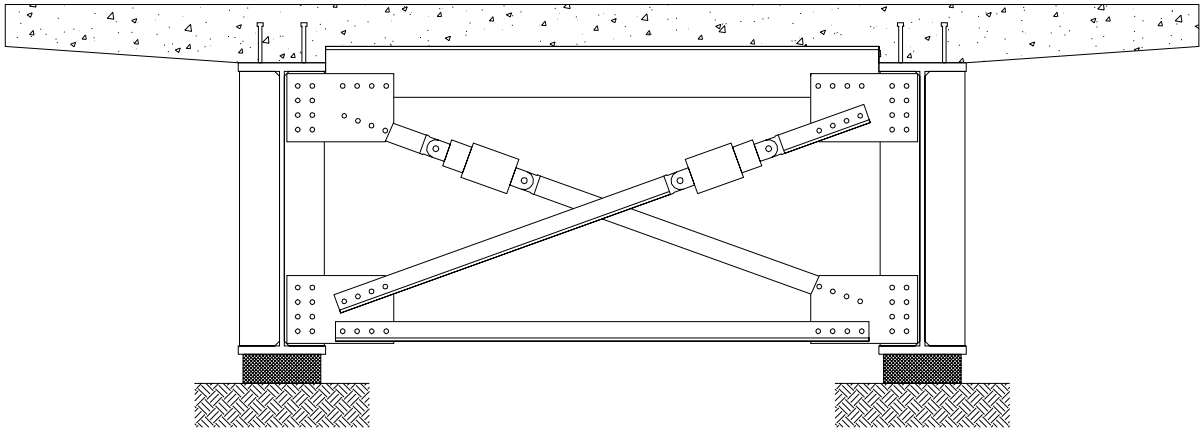

Figure 3.4 Configuration with dampers inserted into existing cross-braces.

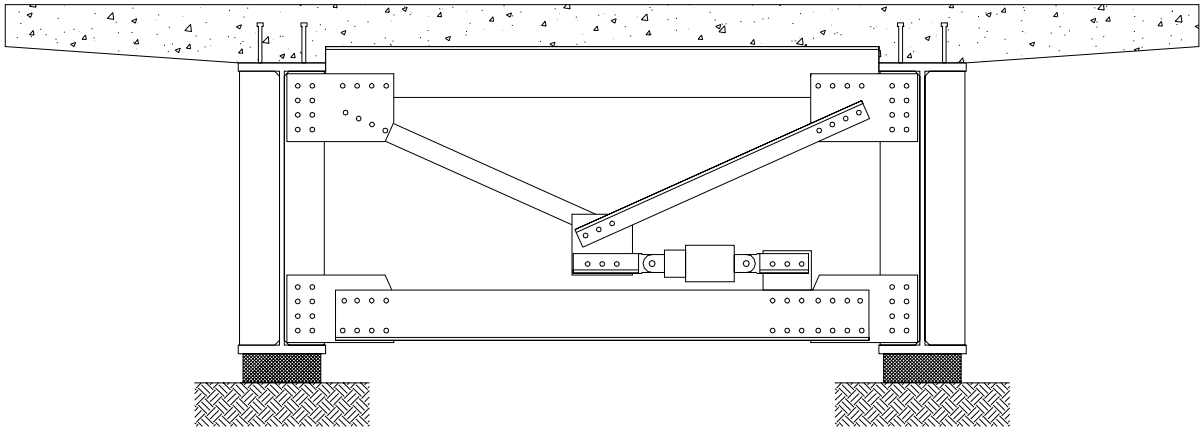

Figure 3.5 Configuration with dampers inserted into chevron cross-braces.

4 RESPONSE OF SCALED MODEL BRIDGE

4.1 Response with Viscous Fluid Dampers

The viscous fluid dampers were used in all three of the device configurations, and performed well in each case. Each configuration was simulated for a range of damper sizes, with damping coefficients ranging from 0.007 kN/mm·s (0.04 kip/in·s) to 17.5 kN/mm·s (100 kip/in·s).

In the cross-brace configuration these dampers were able to significantly improve the response of the bridge superstructure; however, they were able to provide only a marginal decrease in the forces transferred from the superstructure to the abutments.

Figure 4.1 shows the ratio between the displacement of the deck of the controlled bridge and that of the bridge with conventional diaphragms. For the cases with relatively small dampers, the deck displacements increased significantly — by as much as 80%. These increases are due to the stiffness of the structure being greatly decreased, while the dampers do not remove enough energy to compensate for the loss of stiffness. When properly sized dampers were used, the damping forces more than compensated for the stiffness reduction, and the peak displacements were reduced by as much as 80%. The mean reduction with the larger dampers was more that 60%.

Even better response improvements occurred with the shear forces between the deck and the girders. Figure 4.2 shows the ratios of the shear stresses in the end shear connectors —those closest to the abutments. Only in the cases of the smallest dampers

Figure 4.1 Deck displacement ratio with viscous fluid dampers in cross braces.

was there any increase in the shear, while the largest dampers were able to reduce the shears by 90%. These reductions are due to a combination of the energy dissipation in the dampers and the softer response of the less stiff superstructure. The damping forces required to achieve these improvements are shown in Figure 4.3.

Unfortunately, the viscous fluid dampers in the cross-brace configuration could not provide significant reductions in the forces in the bridge bearings and abutments. Figure 4.4 shows the ratio of base shear forces in the bearings at one end of the bridge. As was the case for the shear stress in the shear connectors, there were small increases in the base shear when the dampers were small. Increasing the size of the dampers did not lead to large decreases in the base shear. For the largest dampers, the base shear was reduced by only about 15%, and for the case of the Pacoima Dam earthquake record there was almost no response reduction.

In the chevron brace configuration the viscous fluid dampers performed slightly worse than in the cross brace configuration, and again they did not significantly reduce the forces transferred to the substructure.

The ratio between the deck displacements in the bridges with controlled and conventional diaphragms is shown in Figure 4.5. Again, the reduction in the diaphragm stiffness led to increases in the displacements when the damper were small, but the larger dampers were able to reduce the peak displacements by an average of nearly 60%.

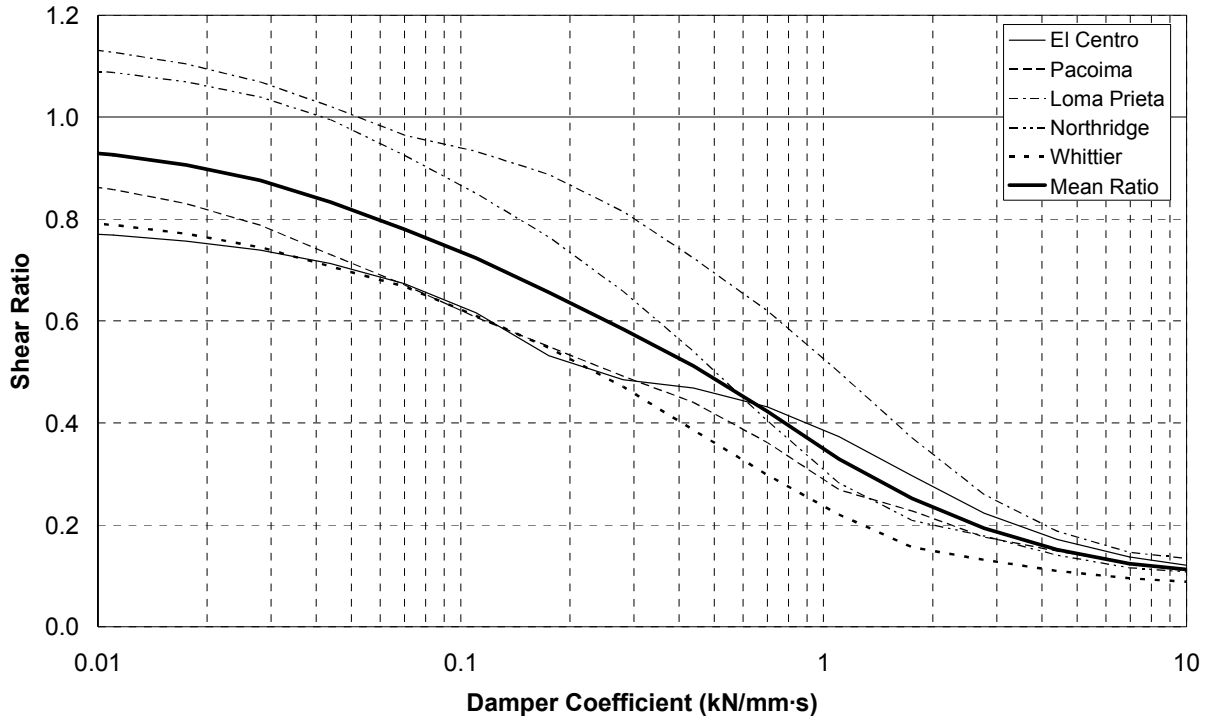

Figure 4.2 Shear Connector stress ratio with viscous fluid dampers in cross braces.

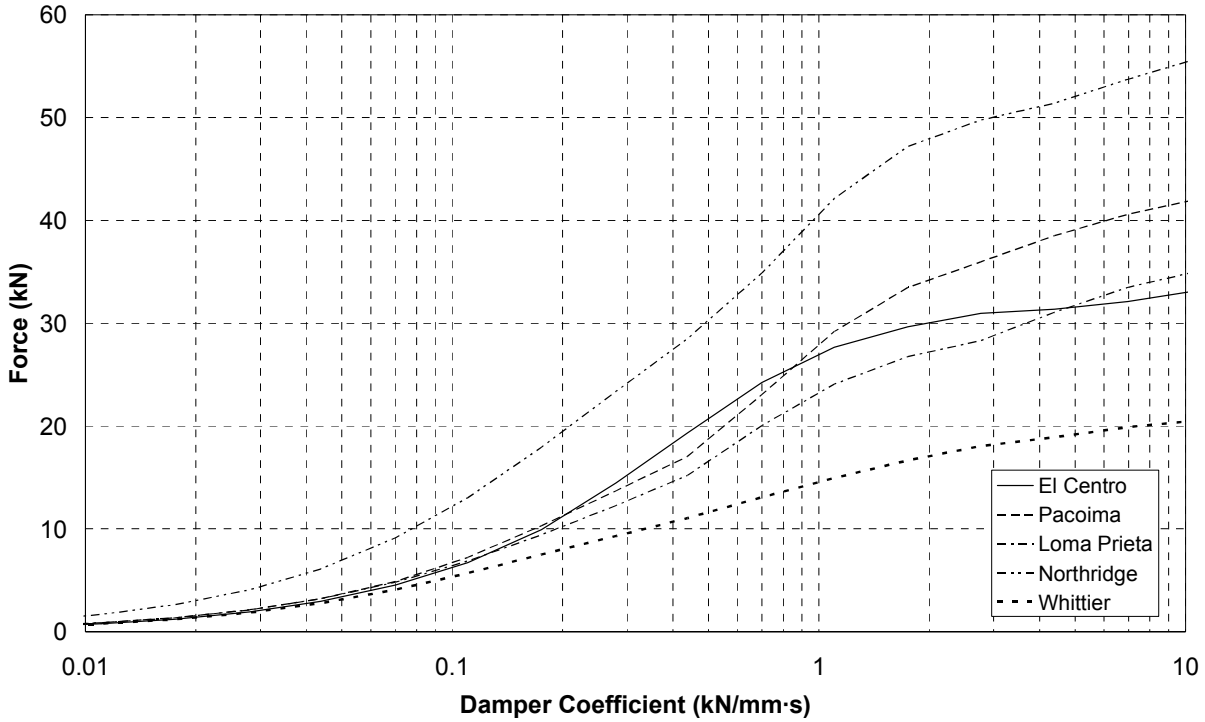

Figure 4.3 Peak forces in viscous fluid dampers in cross braces.

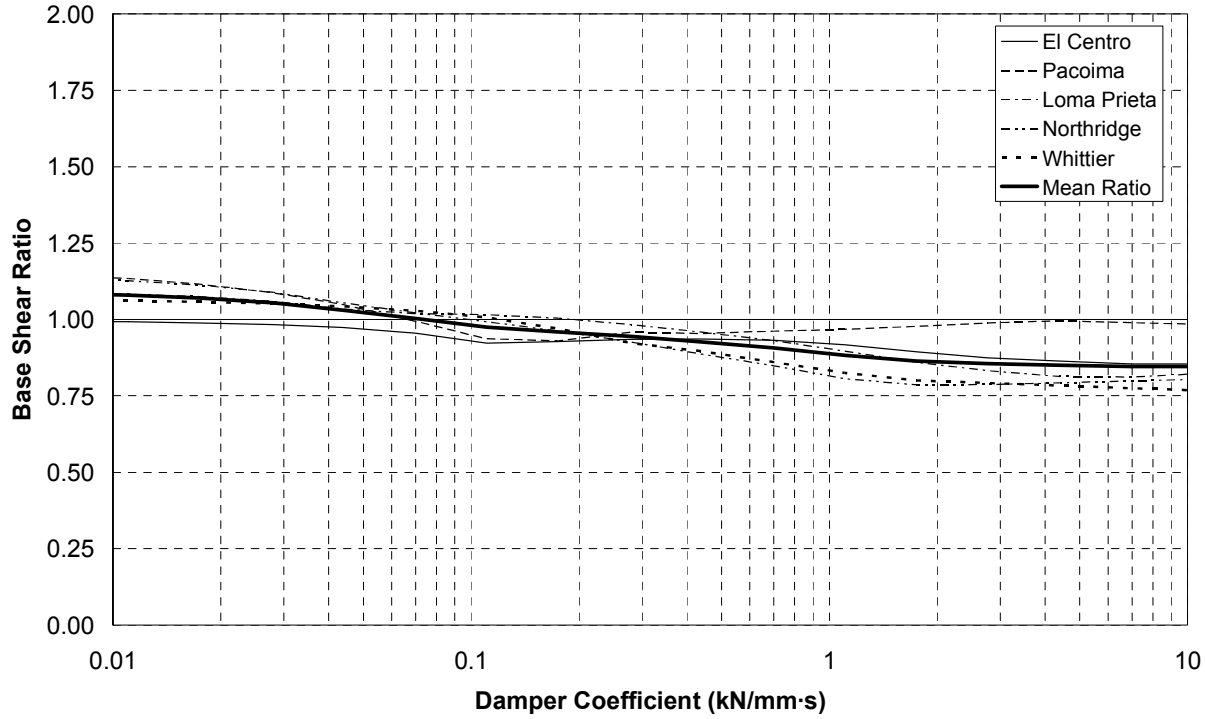

Figure 4.4 Base shear ratio with viscous fluid dampers in cross braces.

The shear forces between the deck and the girders were reduced in nearly all of the cases. Figure 4.6 shows the connector stress ratios between the controlled and conventional cases. Here, the mean reduction during the five earthquake excitations was as great as 80%. The damper forces required to achieve these response improvements are shown in Figure 4.7

As in the case with the dampers in the cross-bracing, the viscous dampers in the chevron-braced configuration had only a limited effect on the shear forces between the girders and abutments. As can be seen in Figure 4.8, the smallest dampers allowed the base shears to increase, while the largest dampers reduced the base shears by an average of 10%.

The third configuration that was considered for the viscous fluid dampers consisted of the dampers connected between the abutments and braces connected to the tops of the girder web stiffeners. This configuration performed poorly compared to the other two.

The displacement responses for this configuration are shown in Figure 4.9. The response with the smallest dampers was similar to the response with the smallest dampers in the chevron brace configuration, but the average improvement with the largest dampers was only about 50%.

In this configuration, even the smallest dampers were able to reduce the peak shear stresses between the girders and the deck by an average of 10%; however, the mean reduction due to the largest dampers was only about 60%. This is, of course, an impressive improvement in the structural response, but it is small in comparison to the improvements achieved by the cross-braced and chevron-braced configurations.

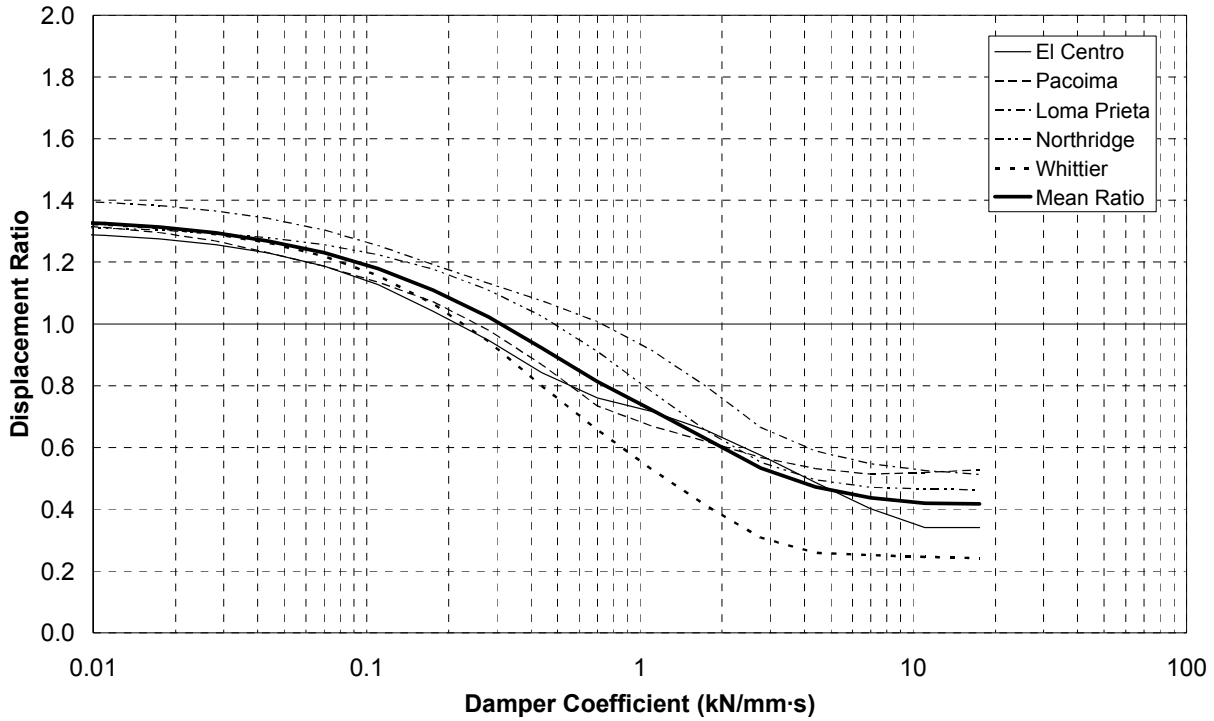

Figure 4.5 Deck displacement ratio with viscous fluid dampers in chevron braces.

The peak damper forces are shown in Figure 4.11. These forces are significant because in this configuration they are being transmitted directly to the abutments. Figure 4.12 shows the ratios between the peak base shear forces of the damped and conventional diaphragm cases. In this configuration, best improvements in the base shear response occur with the medium sized dampers. The increased base shears that occur with the large dampers are directly due to the large damping forces. In fact, the forces transmitted through the bridge bearings are significantly reduced by the largest dampers in this configuration.

In all three brace configurations, the viscous fluid dampers were able to significantly improve the response of the superstructure, with the cross-brace configuration providing the best improvements. The configuration that connects the dampers directly to the abutments has good potential for cases where the substructure has adequate reserve strength, but where the bearing strength is limited. Unfortunately, none of these configurations are appropriate when the substructure is inadequate for the seismic loads.

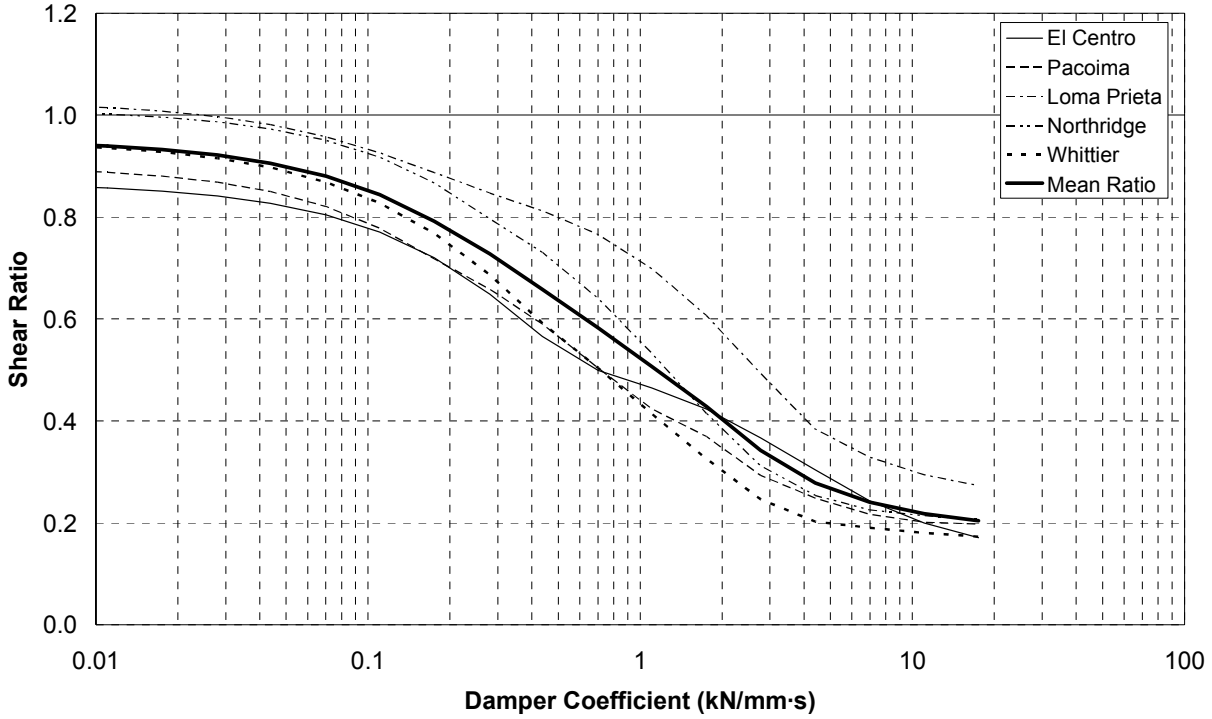

Figure 4.6 Shear connector stress ratio with viscous fluid dampers in chevron braces.

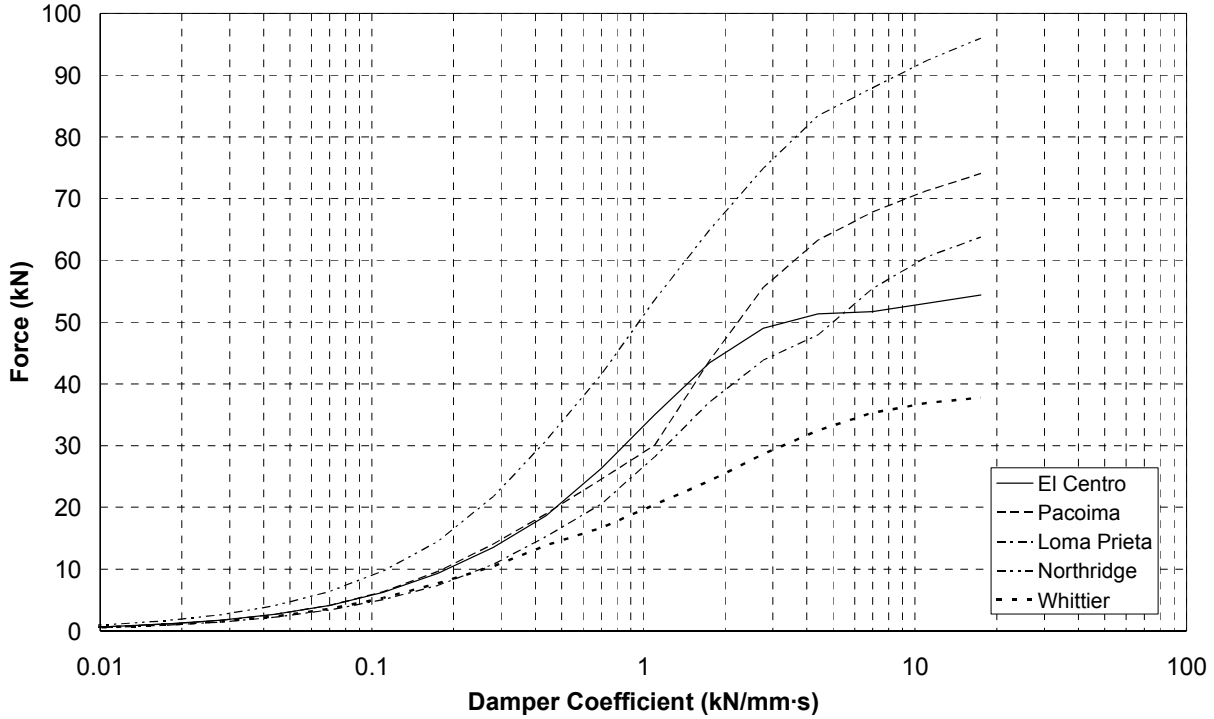

Figure 4.7 Peak forces in viscous fluid dampers in chevron braces.

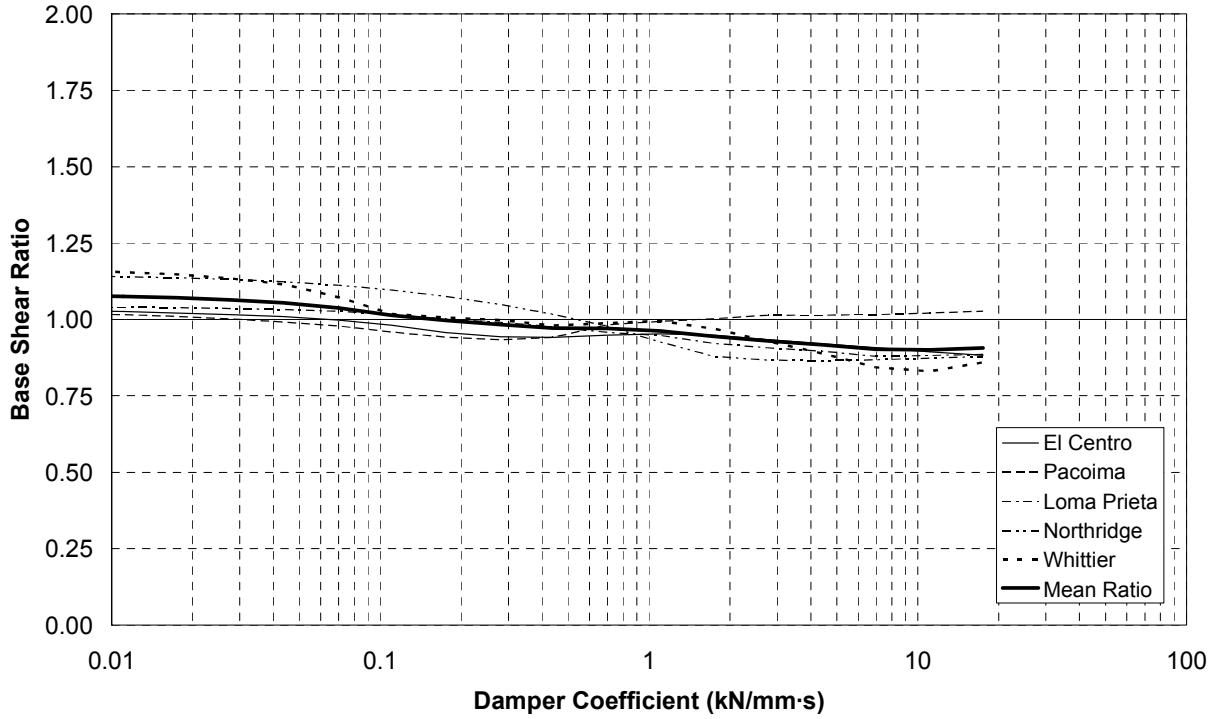

Figure 4.8 Base shear ratio with viscous fluid dampers in chevron braces.

Figure 4.9 Deck displacement ratio with viscous fluid dampers connected to abutments.

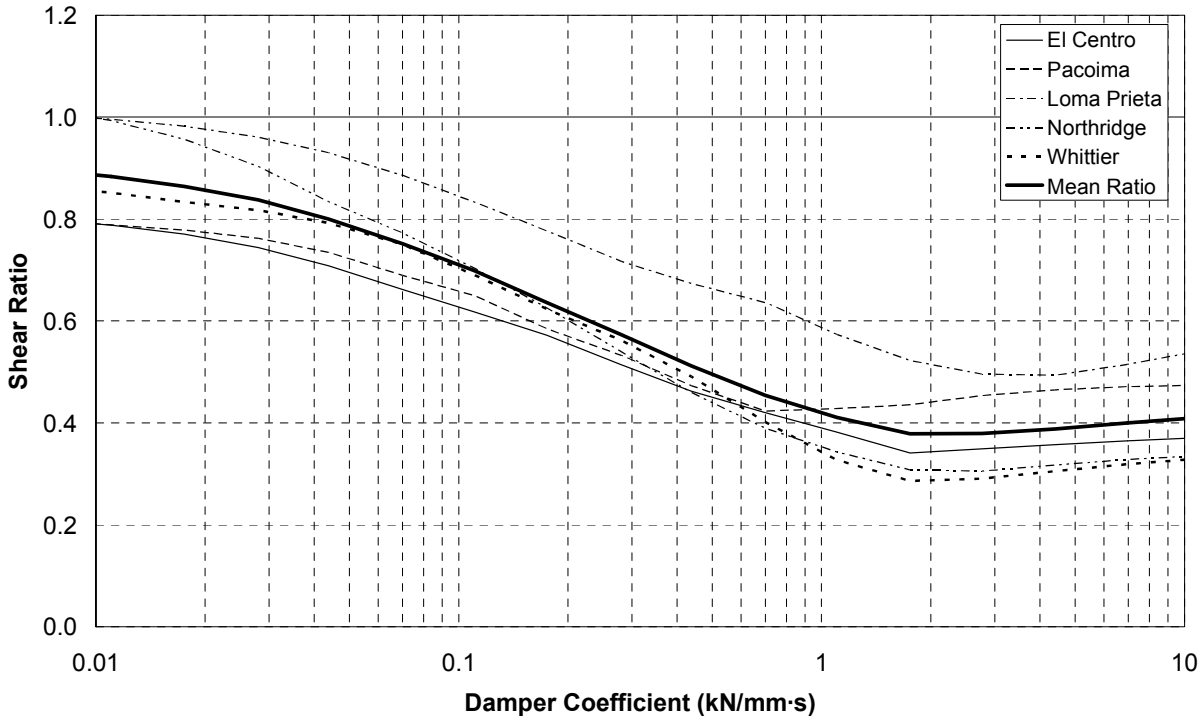

Figure 4.10 Shear connector stress ratio with VF dampers connected to abutments.

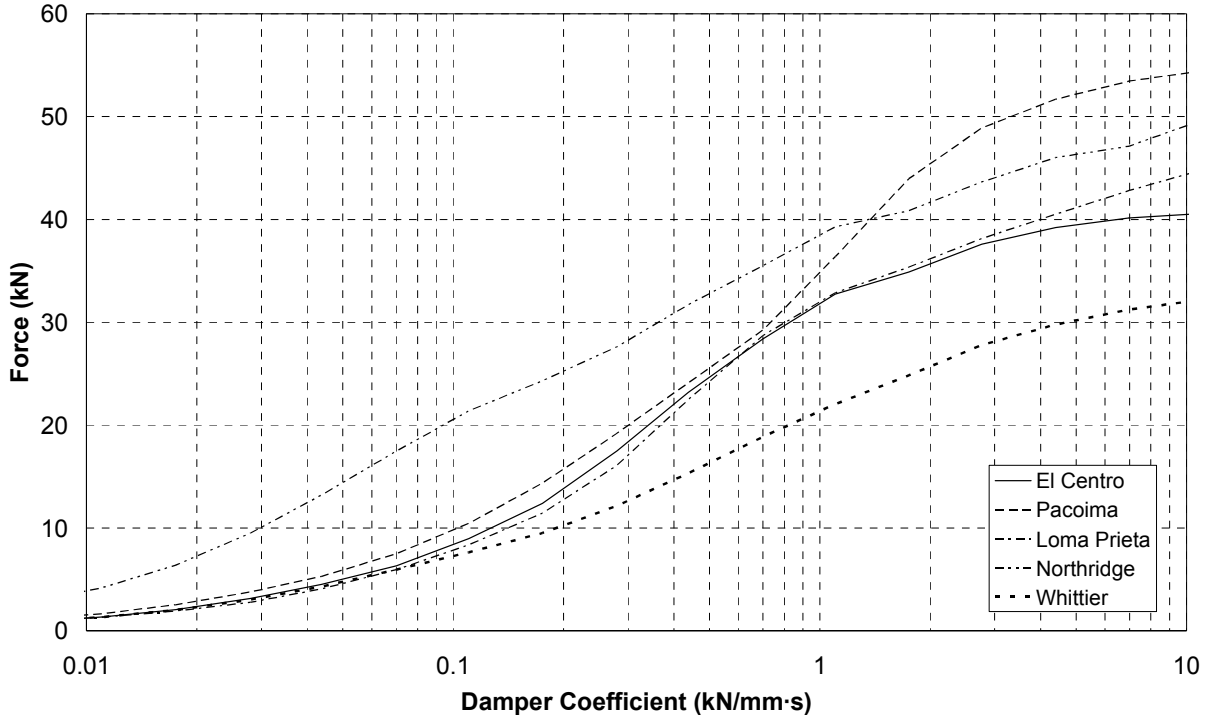

Figure 4.11 Peak forces in viscous fluid dampers connected to abutments.

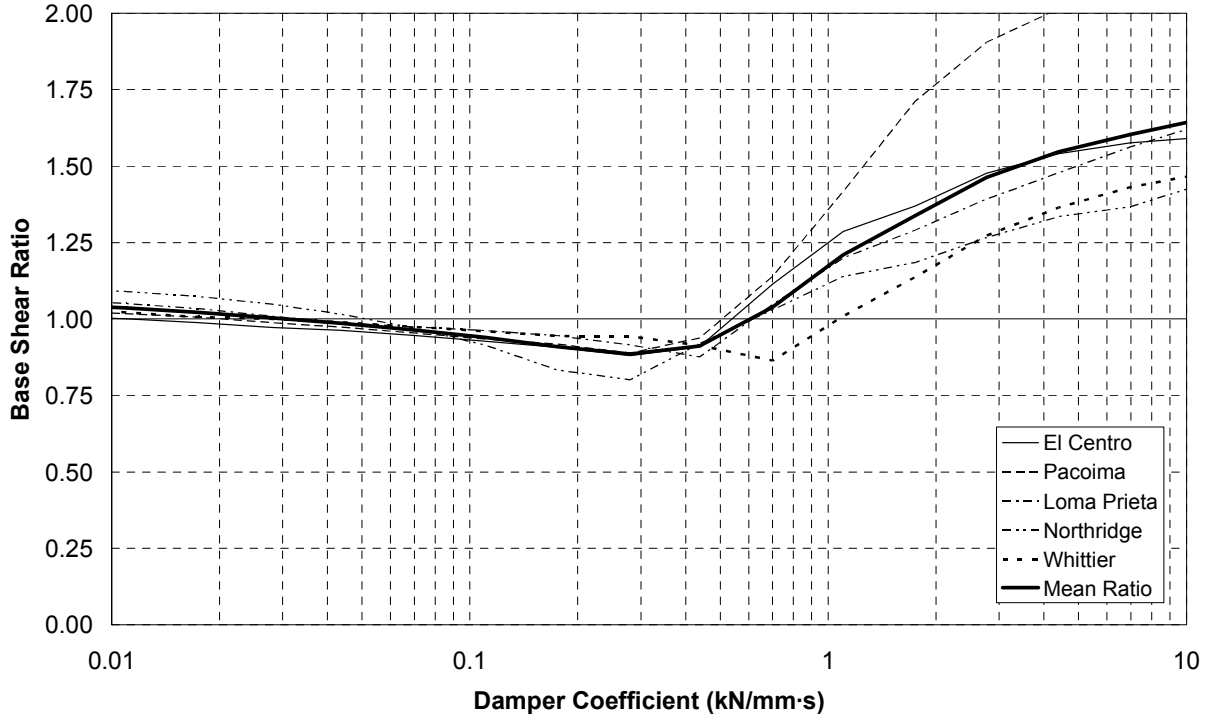

Figure 4.12 Base shear ratio with viscous fluid dampers connected to abutments.

4.2 Response with Friction Dampers

Friction dampers were used in all three brace configurations and performed acceptably in each. However, these dampers tended to perform poorly as compared to the viscous fluid dampers. The response was simulated for dampers with slip forces ranging from 0.445 kN (0.1 kip) to 445 kN (100 kip).

The response with the friction dampers in the cross-brace configuration is shown in Figure 4.13 through Figure 4.16. While the smallest dampers performed poorly, allowing the displacements and shear forces to increase, the medium sized dampers were able to significantly improve the response of the bridge. As the dampers became larger, the response forces were not large enough to activate the dampers, and the bridge responses approached those of the bridge with conventional diaphragms.

The best responses occurred for dampers with slip forces of 30 kN to 45 kN, representing 40% to 60% of the tributary weight of the superstructure. With these dampers, the average of the peak deck displacements was reduced by more than 30% and the average of the peak shear forces between the deck and girders was reduced by more than 40%. However, the base shear was only reduced about 5%.

The response with the friction dampers in the chevron-brace configuration was similar to the response in the cross-brace configuration. As can be seen in Figure 4.17 through Figure 4.20, the smallest dampers had little impact on the response, while the largest ones were not activated and instead acted as rigid struts.

The dampers with slip forces between 20 kN and 45 kN performed best, with a slip force equal to about 35% of the tributary weight appearing to be optimal for this configuration. In this case, the displacements were reduced by an average of 15% and the shear between the deck and the girders by about 25%. This configuration had no impact on the base shear forces.

The final configuration for the friction dampers was with the dampers connected directly to the bridge abutments. The response with this configuration, shown in Figure 4.21 through Figure 4.24, tended to be somewhat better than the response with either the cross brace or chevron brace configurations.

In this configuration, the best damper slip force varied with the response of interest. The displacements were reduced the most with damper slip forces between 45 kN and 70 kN. These dampers reduced the average response by about 50%. The shear forces between the deck and girders were reduced the most by dampers with slip forces between 30 kN and 45 kN. In these cases the response was reduced by more than 40%. The average of the peak base shears was reduced by 20% by dampers with slip forces between 10 kN and 20 kN. Larger dampers significantly increased the base shear forces.

As in the case of the viscous fluid dampers, the friction dampers were able to improve the response of the superstructure in all three brace configurations. However, the response improvements tended to be smaller than with the fluid dampers. The major advantage to using friction devices instead of the fluid dampers would be the cost of the devices, which could make the friction devices more practical for many retrofit situations.

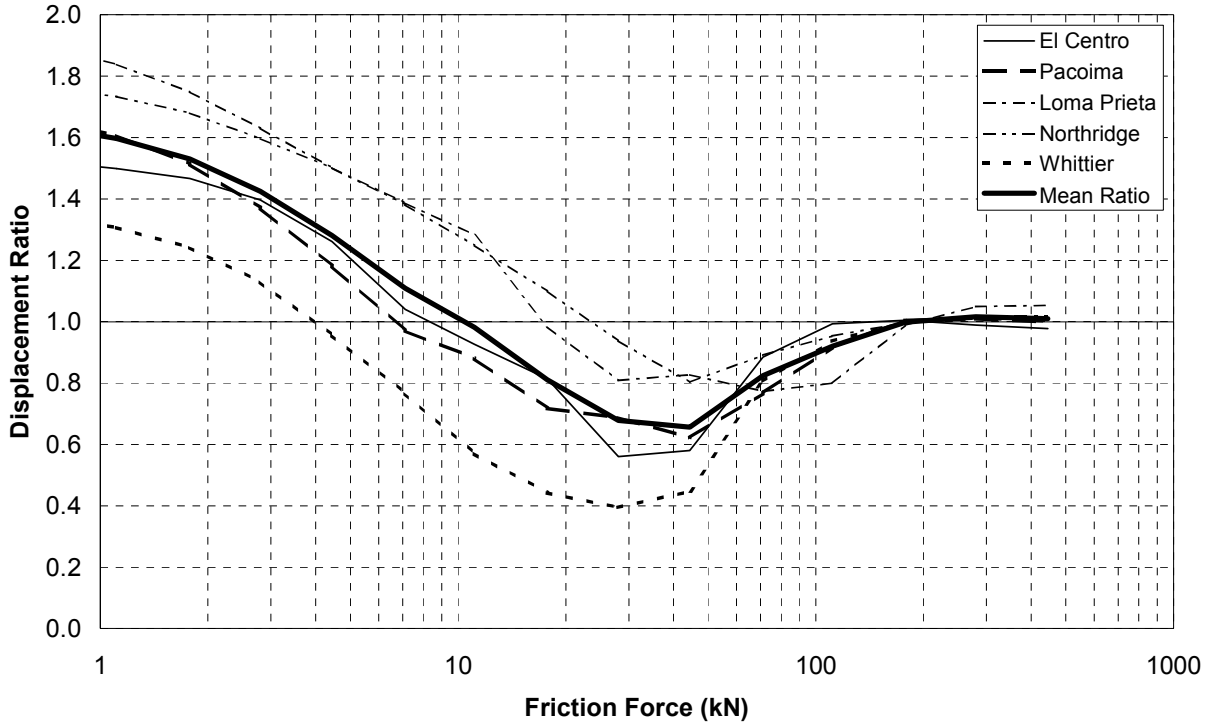

Figure 4.13 Deck displacement ratio with friction dampers in cross braces.

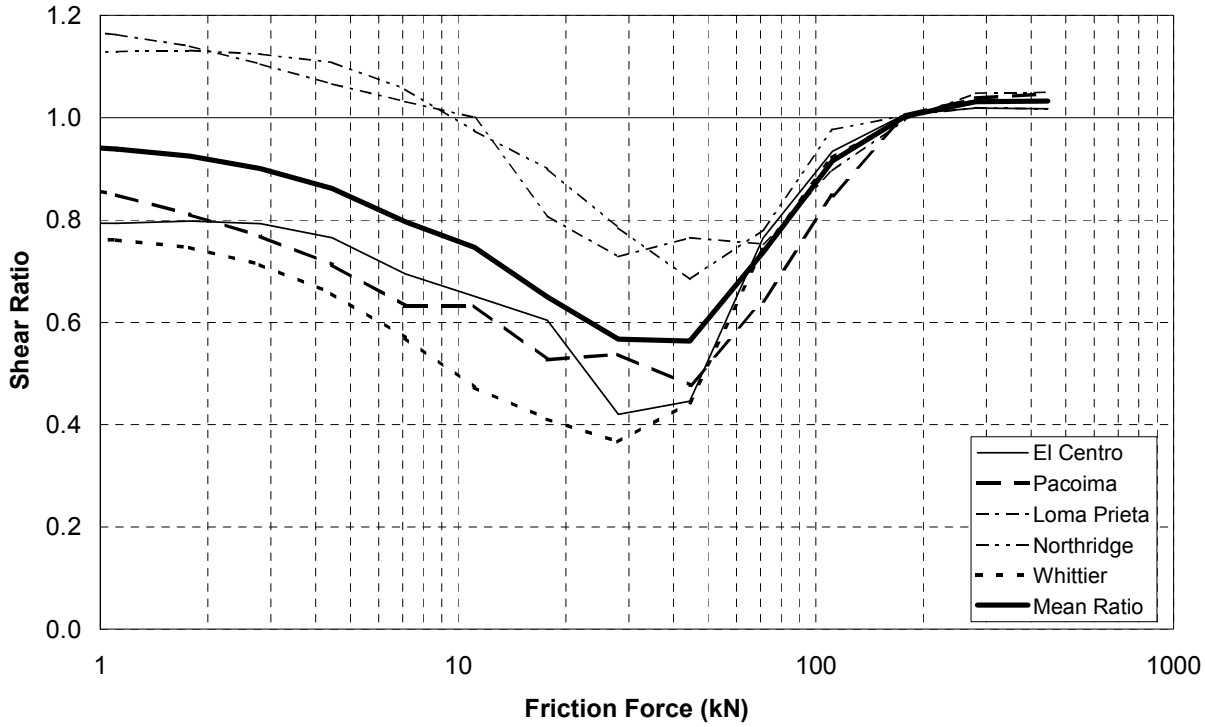

Figure 4.14 Shear connector stress ratio with friction dampers in cross braces.

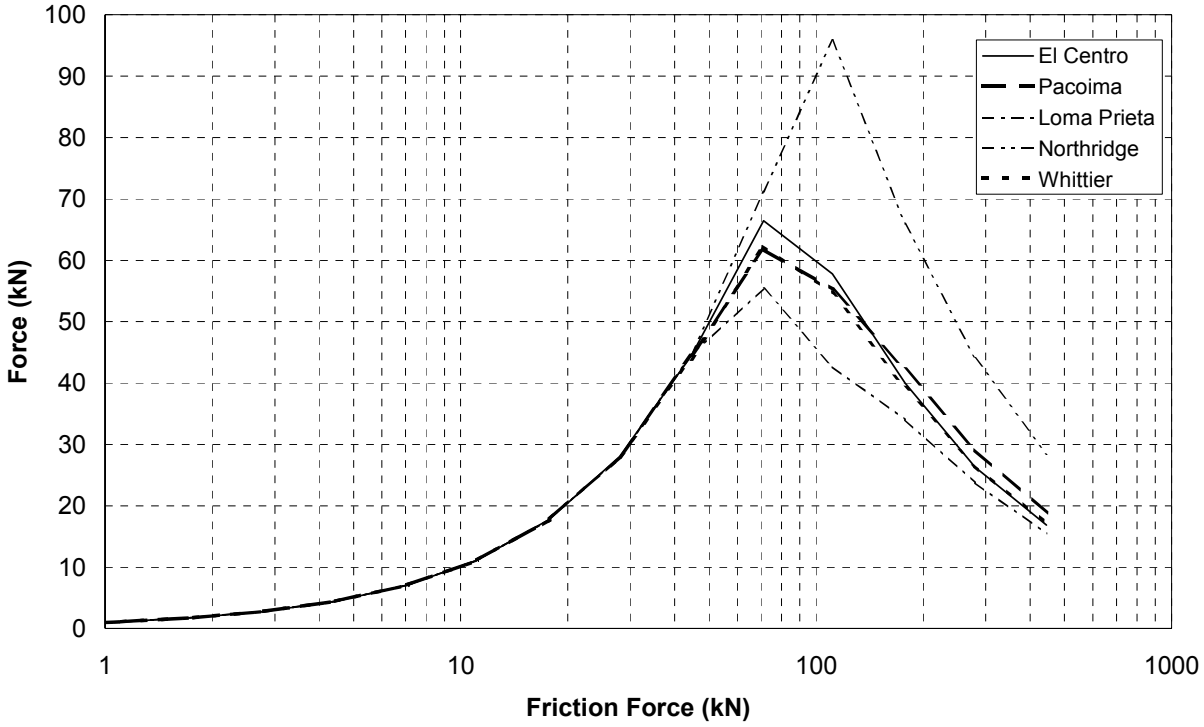

Figure 4.15 Peak forces in friction dampers in cross braces.

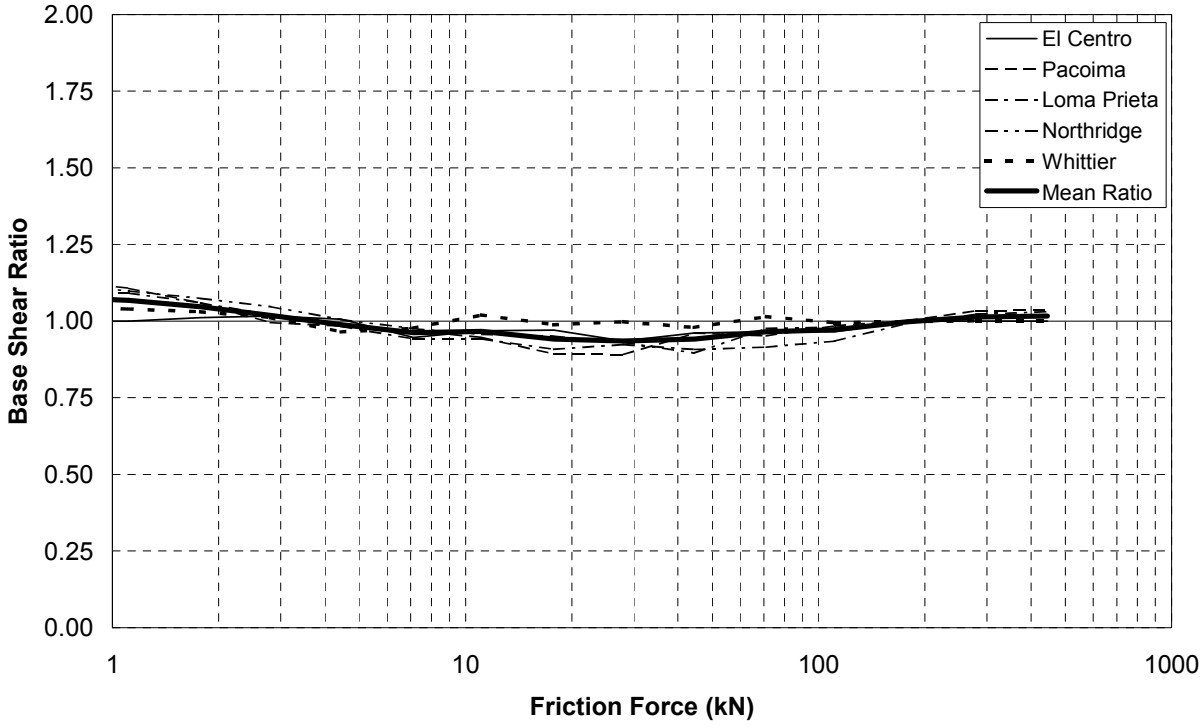

Figure 4.16 Base shear ratio with friction dampers in cross braces.

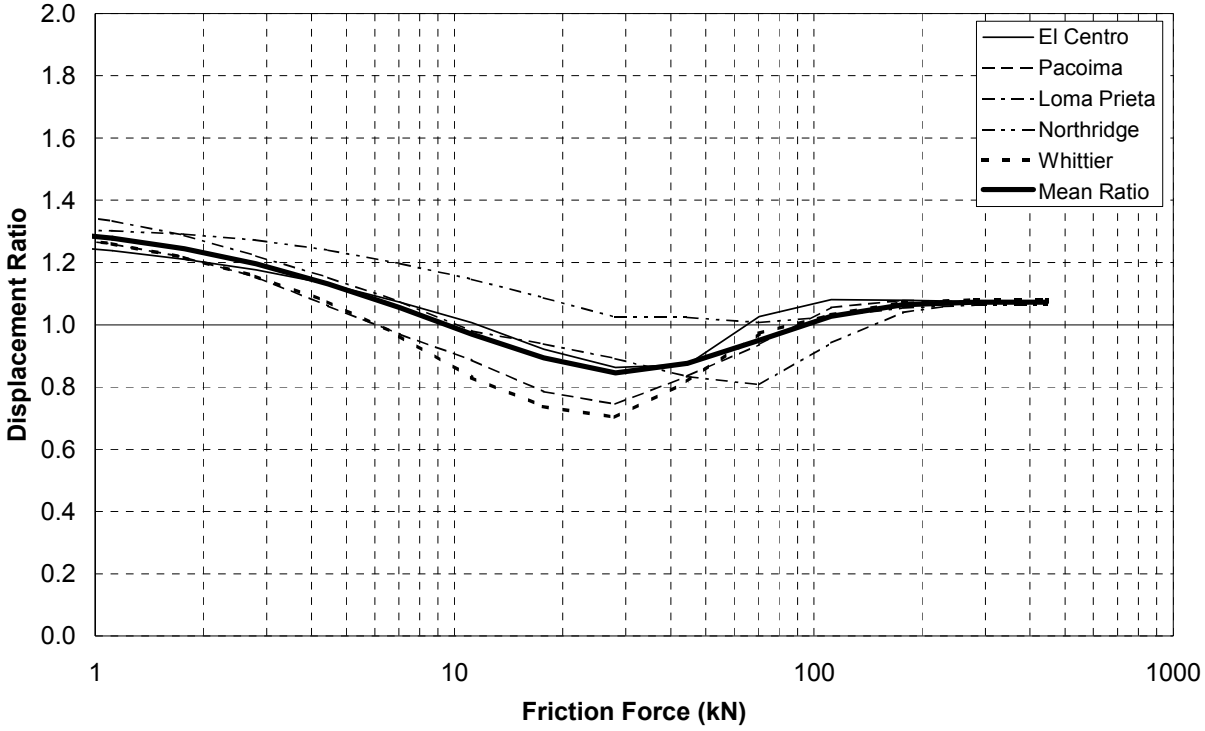

Figure 4.17 Deck displacement ratio with friction dampers in chevron braces.

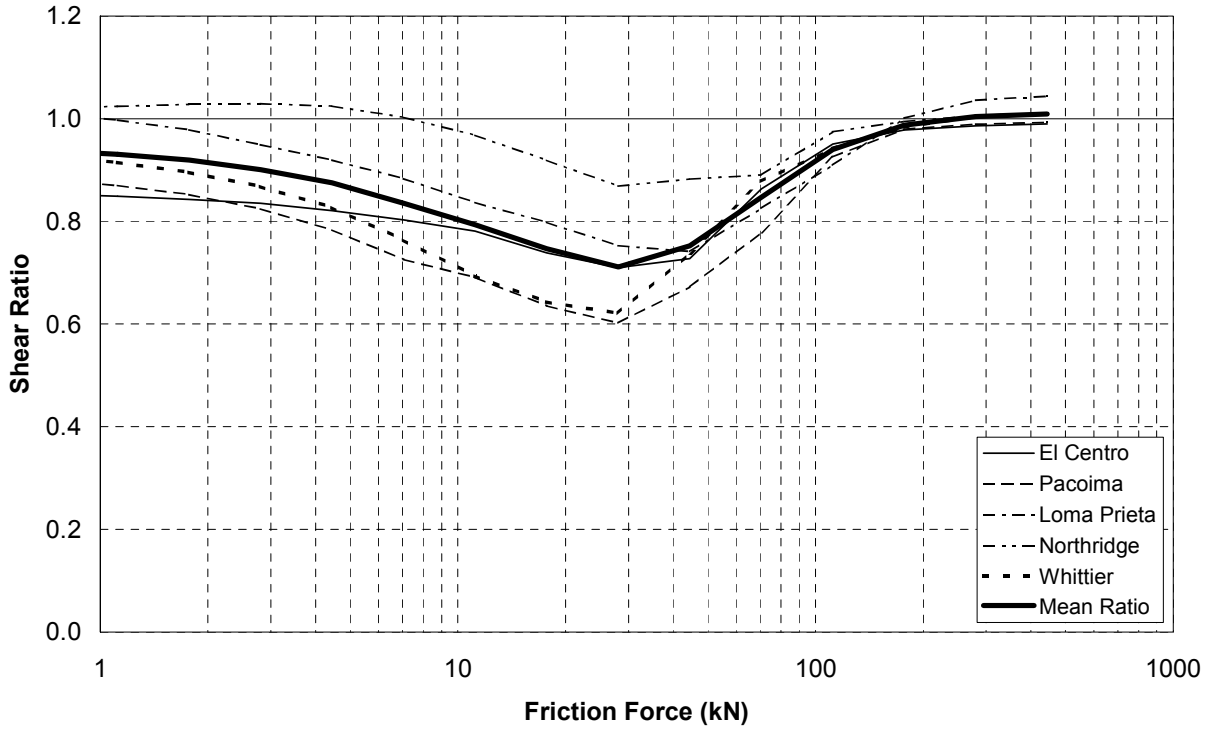

Figure 4.18 Shear connector stress ratio with friction dampers in chevron braces.

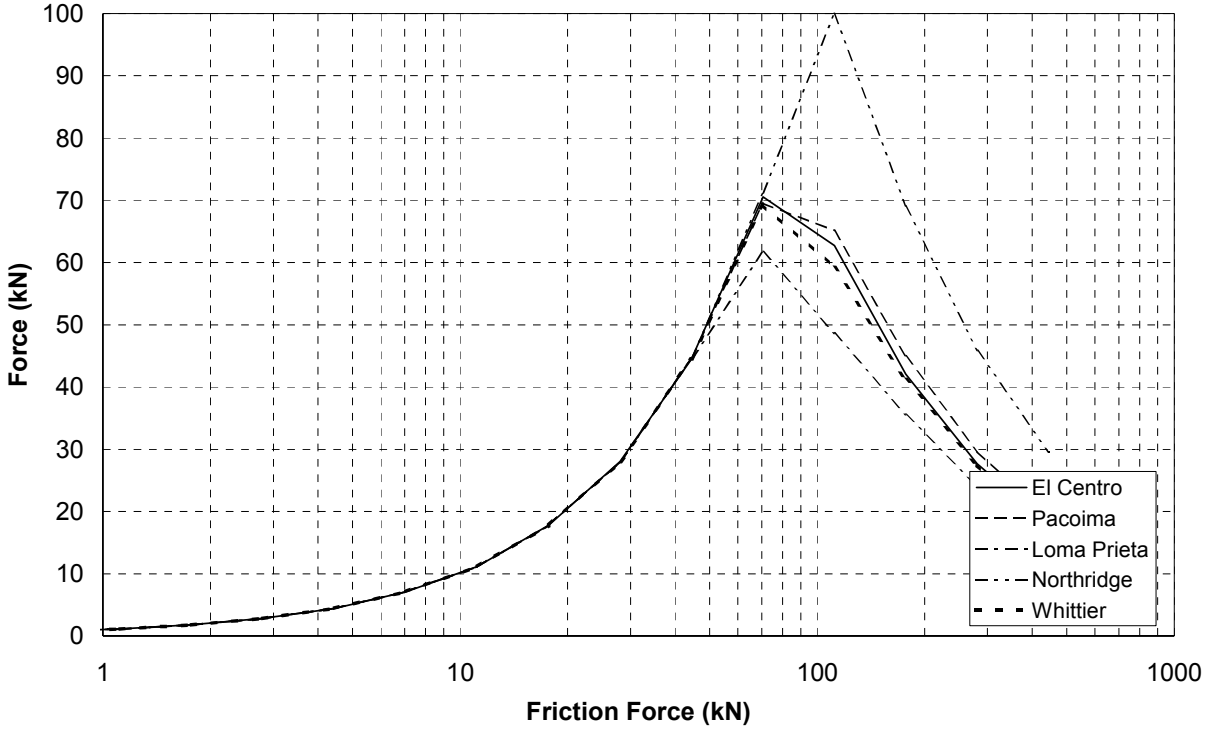

Figure 4.19 Peak forces in friction dampers in chevron braces.

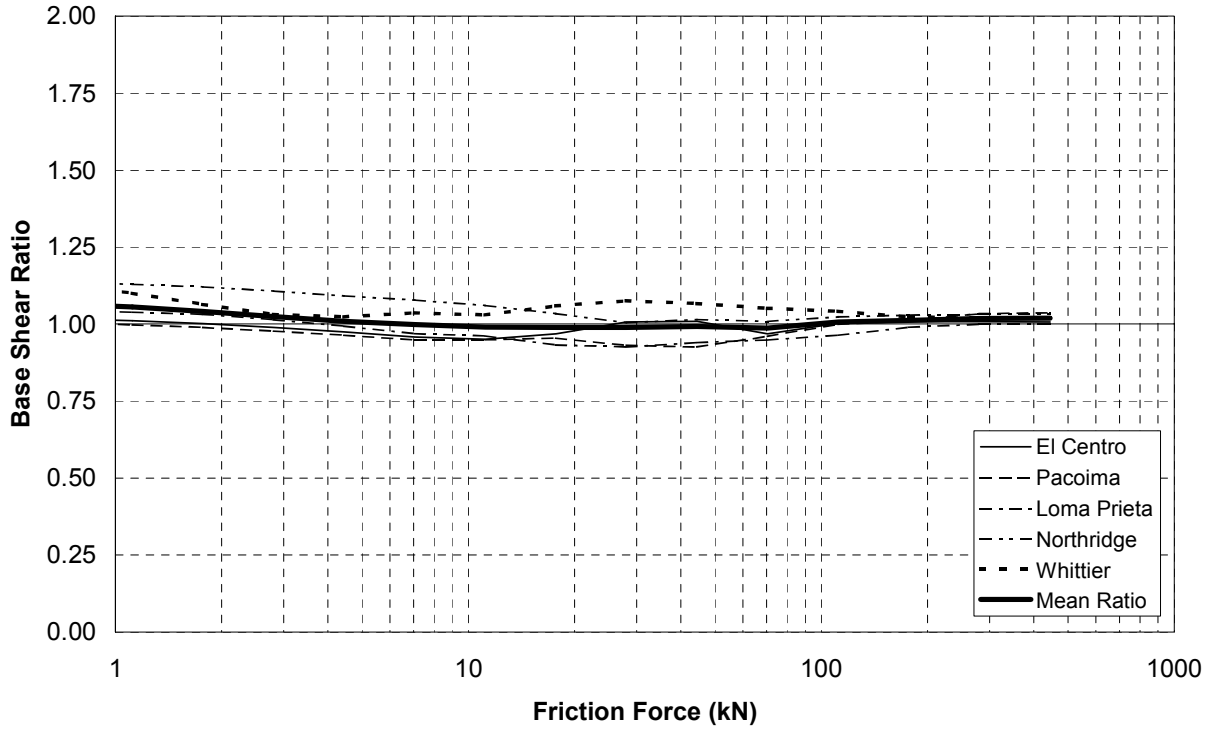

Figure 4.20 Base shear ratio with friction dampers in chevron braces.

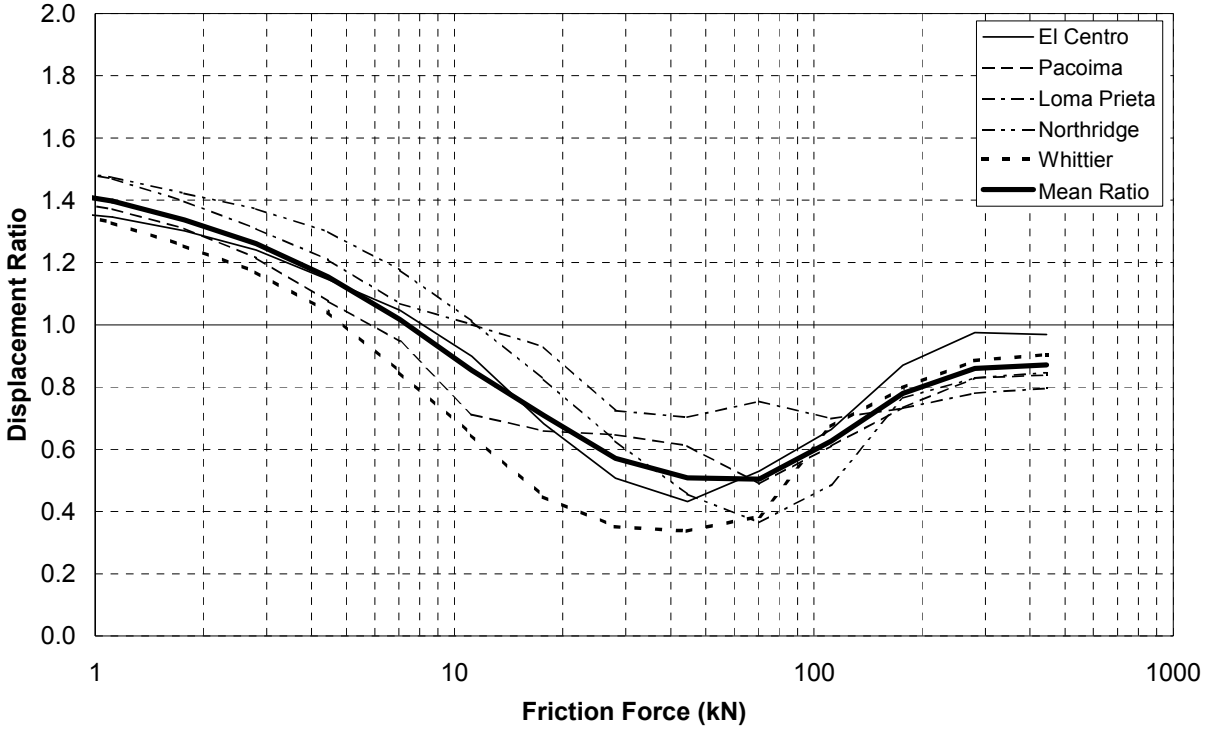

Figure 4.21 Deck displacement ratio with friction dampers connected to abutments.

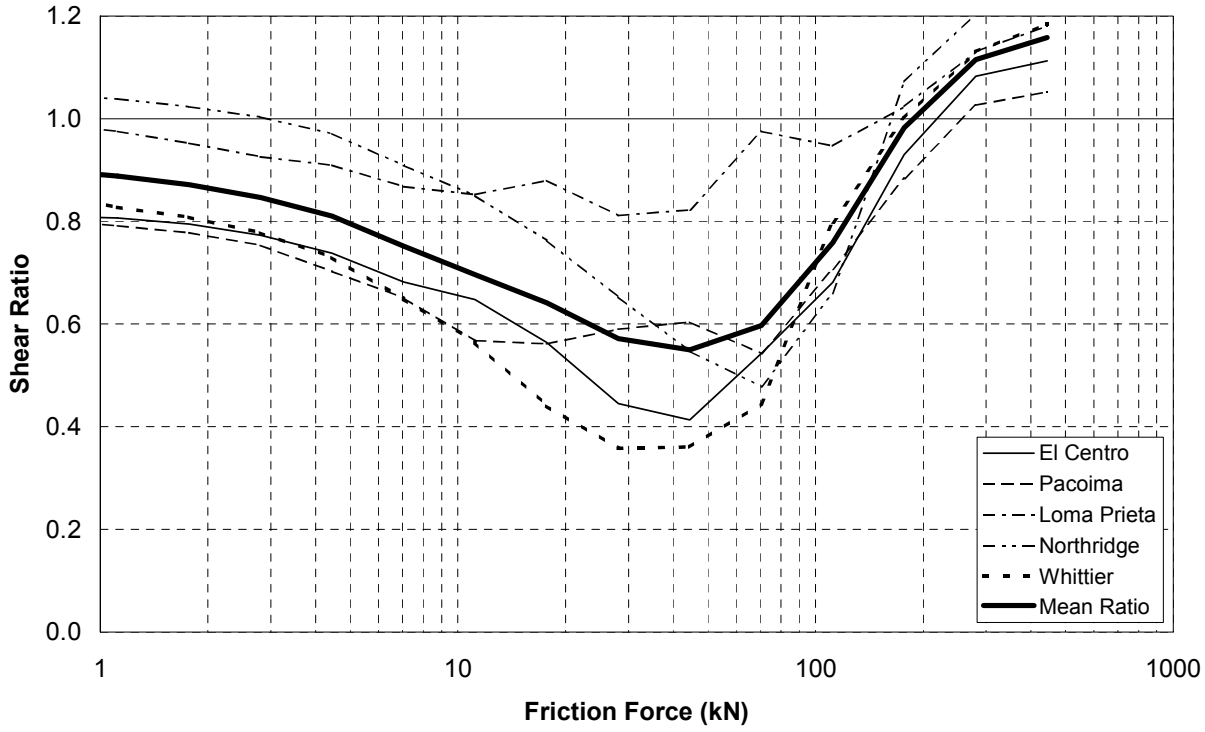

Figure 4.22 Shear connector stress ratio with friction dampers connected to abutments.

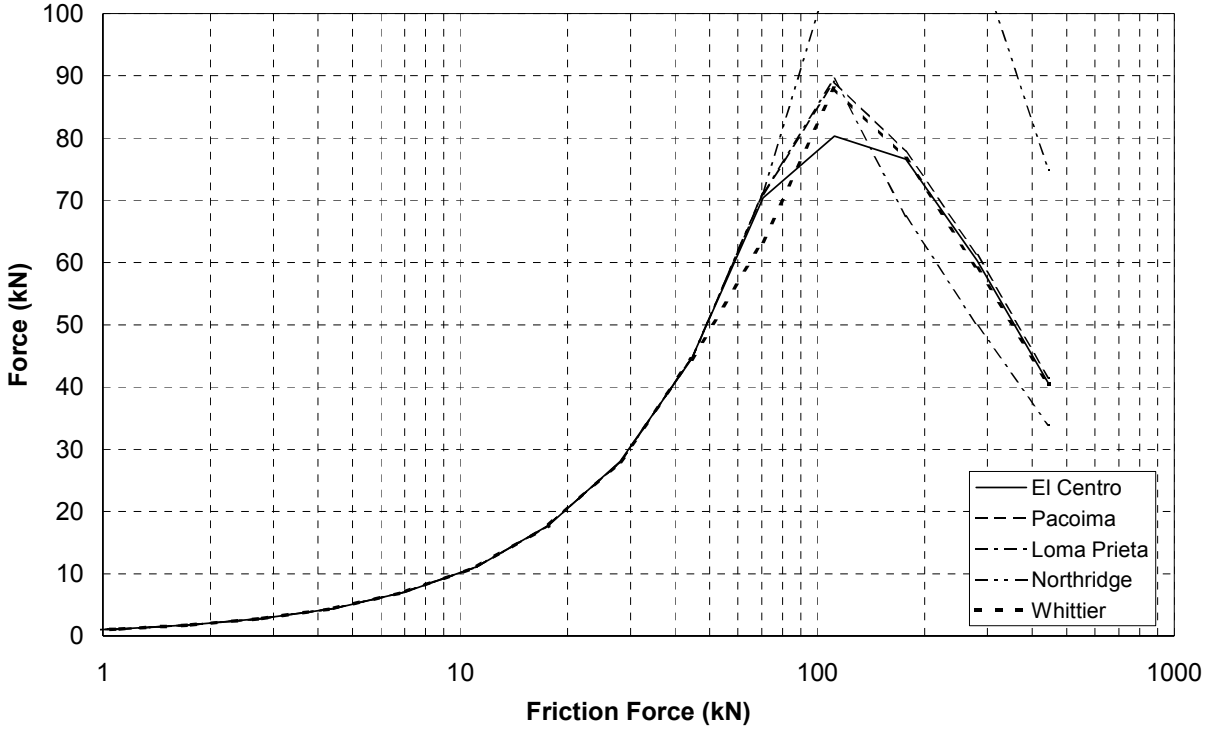

Figure 4.23 Peak forces in friction dampers connected to abutments.

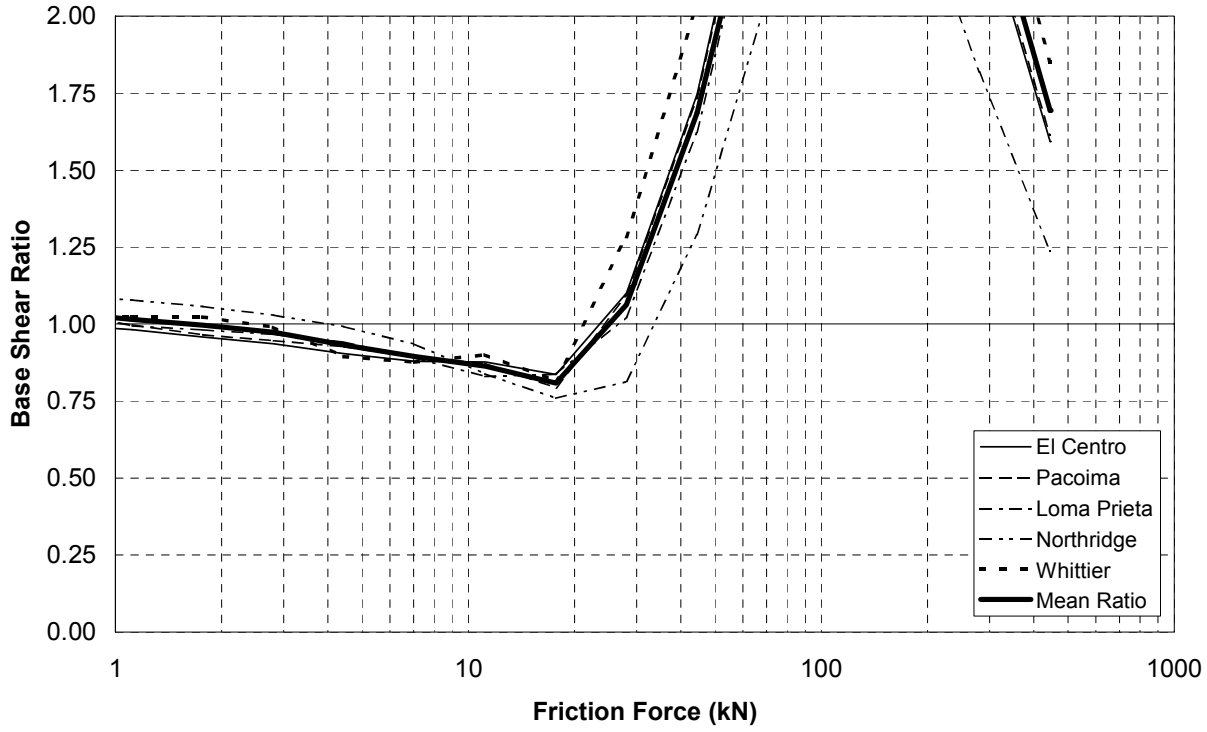

Figure 4.24 Base shear ratio with friction dampers connected to abutments.

4.3 Response with Viscoelastic Dampers

The viscoelastic (VE) dampers were used in two brace configurations, the chevron braces and braces directly connected to the abutments. These devices performed acceptably in both configurations, but the resulting response was not as good as with the viscous fluid dampers and was mixed as compared to the friction dampers.

A single type of viscoelastic material was chosen for the simulations. The material had a shear storage modulus of 965 kPa (140 psi) and a shear loss modulus of 1165 kPa (169 psi). This led to a series of dampers that all had a constant ratio of 8.2 between the damping coefficient and stiffness. Dampers were simulated with damping coefficients ranging from 0.007 kN/mm·s (0.04 kip/in·s) to 17.5 kN/mm·s (100 kip/in·s), and the associated stiffness ranging from 0.058 kN/mm (0.33 kip/in) to 144 kN/mm (823 kip/in).

In the chevron brace configuration, the smallest of these dampers performed similarly to the viscous fluid devices, but as the size of the VE devices increased, the stiffness component of the device response became significant and these devices improved the response less. The most efficient dampers, with damping coefficients between 2 kN/mm·s and 3 kN/mm·s, were able to reduce the deck displacements by an average of 20%, as shown in Figure 4.25. These devices were also able to reduce the shear forces between the deck and the girders by 30%, as shown in Figure 4.26.

The VE dampers in this configuration had little impact on the base shear forces, as shown in Figure 4.27. The peak damping and stiffness components of the damper forces are shown in Figure 4.28 and Figure 4.29, respectively.

Figure 4.25 Deck displacement ratio with VE dampers in chevron braces.

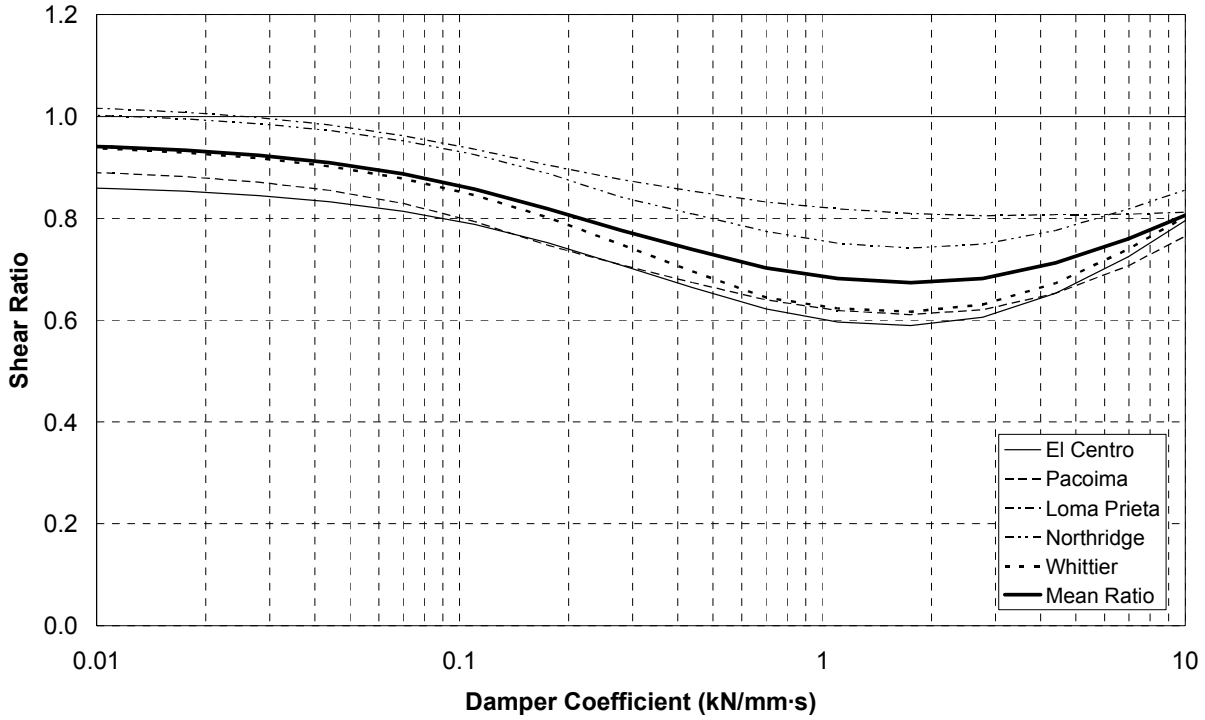

Figure 4.26 Shear connector stress ratio with VE dampers in chevron braces.

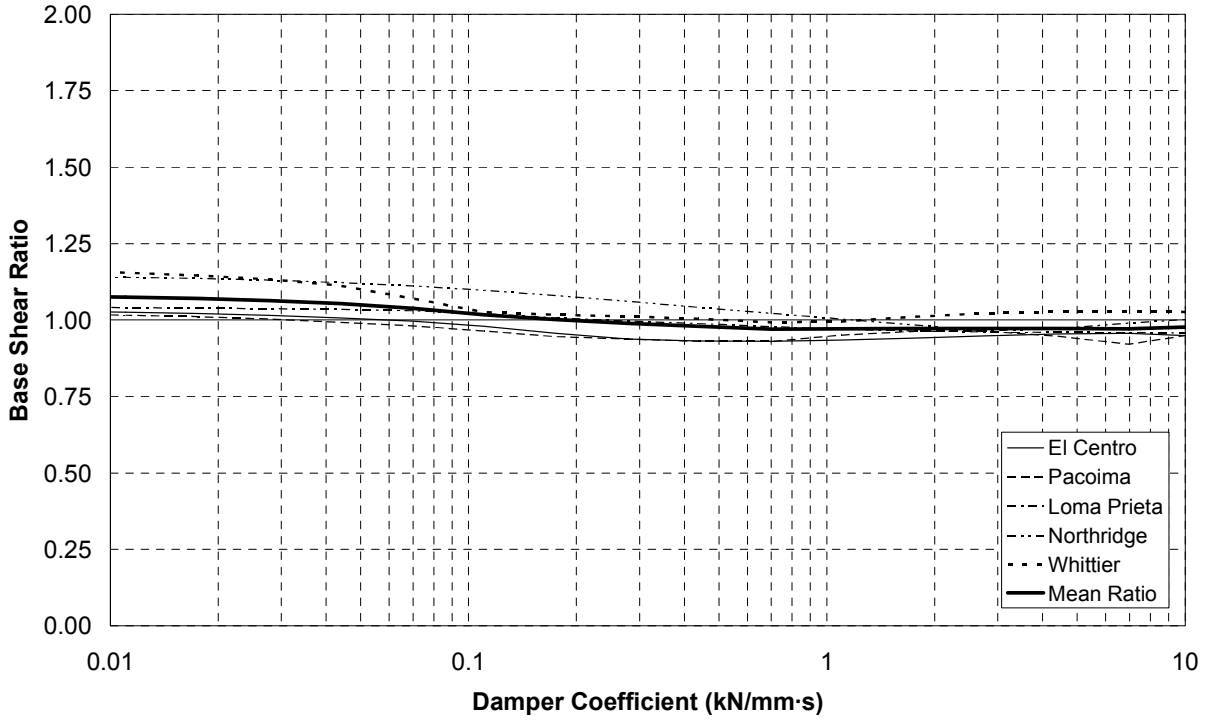

Figure 4.27 Base shear ratio with VE dampers in chevron braces.

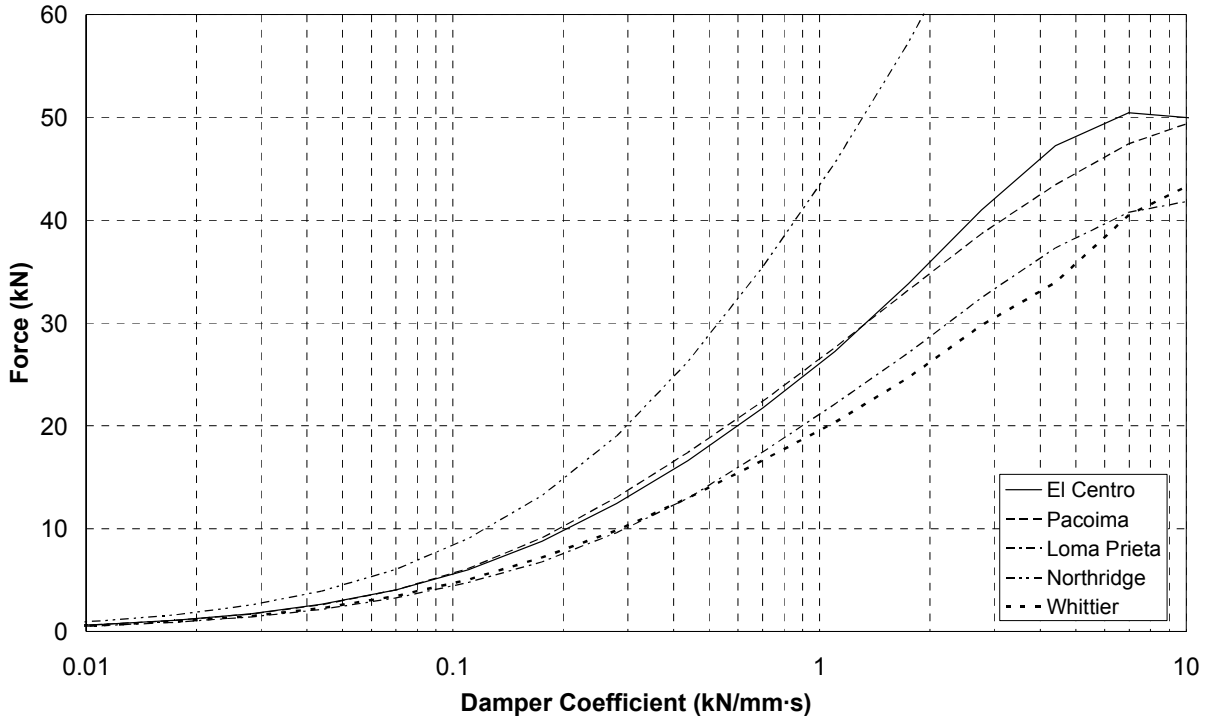

Figure 4.28 Peak damping forces in VE dampers in chevron braces.

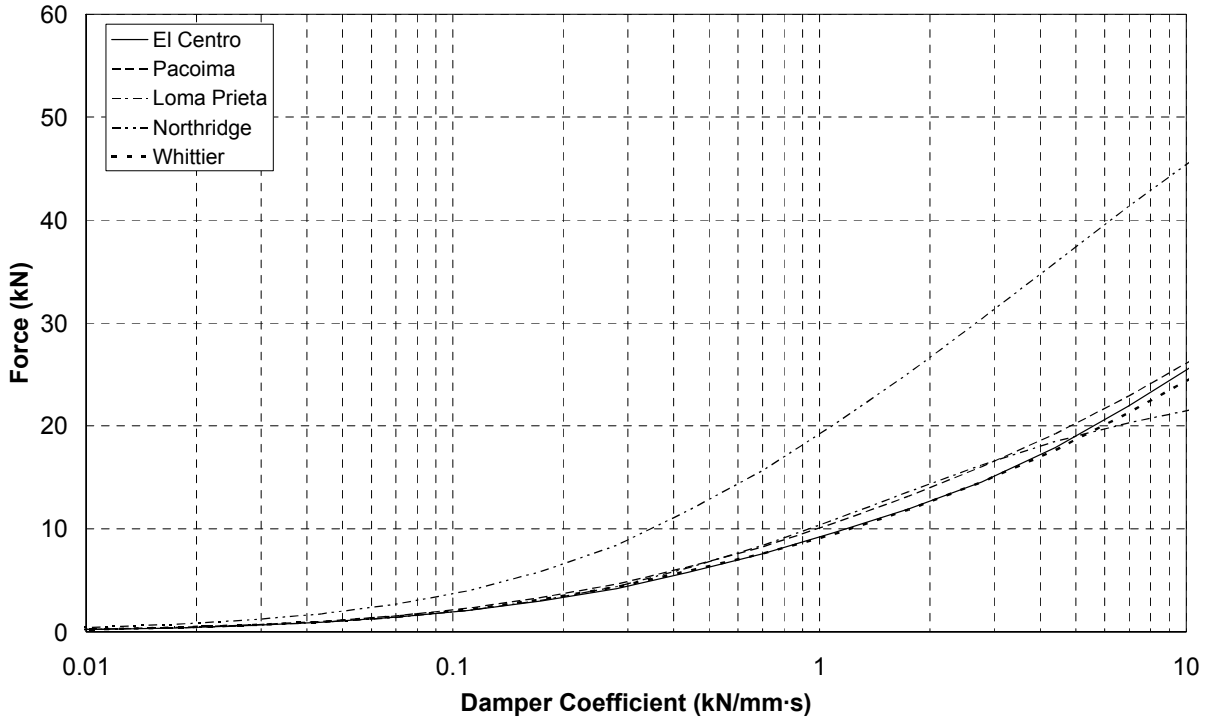

Figure 4.29 Peak stiffness forces in VE dampers in chevron braces.

When the VE dampers were connected directly to the abutments they performed slightly better and the best response was provided by smaller dampers. In this configuration, VE dampers with damping coefficients between 0.7 kN/mm·s and 1.1 kN/mm·s were able to reduce the peak deck displacements by an average of about 25%, as shown in Figure 4.30. Similarly, devices with damping coefficients between 0.2 kN/mm·s and 0.7 kN/mm·s were able to reduce the peak shear forces between the deck and the girders by about 33%. This response is shown in Figure 4.31.

The most effective dampers were able the base shear forces by an average of 20%, as shown in Figure 4.32. As was the case with the viscous fluid dampers and friction devices, the minimum base shear occurred just before the damper forces, shown in Figure 4.33 and Figure 4.34, became the most significant portion of the total base shear. When the damper forces are excluded from the base response, the remaining forces, which are due to the shear in the bearings, continue to decrease as the damper size increases.

As in the case of the viscous fluid and friction dampers, the viscoelastic dampers were able to improve the response of the superstructure in all three brace configurations. However, like the friction dampers, the response improvements tended to be smaller than with the fluid dampers. Due to the viscoelastic material's temperature dependence and no strongly compelling performance advantage, these devices are judged not to be practical for use in highway bridges.

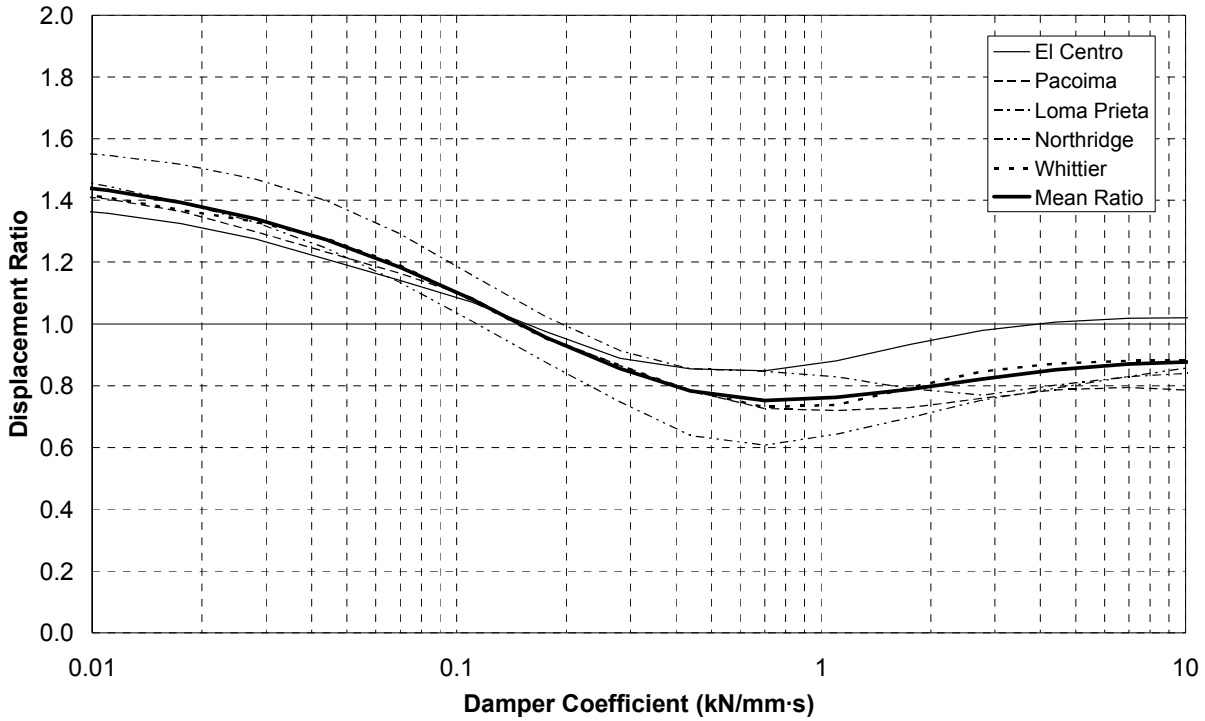

Figure 4.30 Deck displacement ratio with VE dampers connected to abutments.

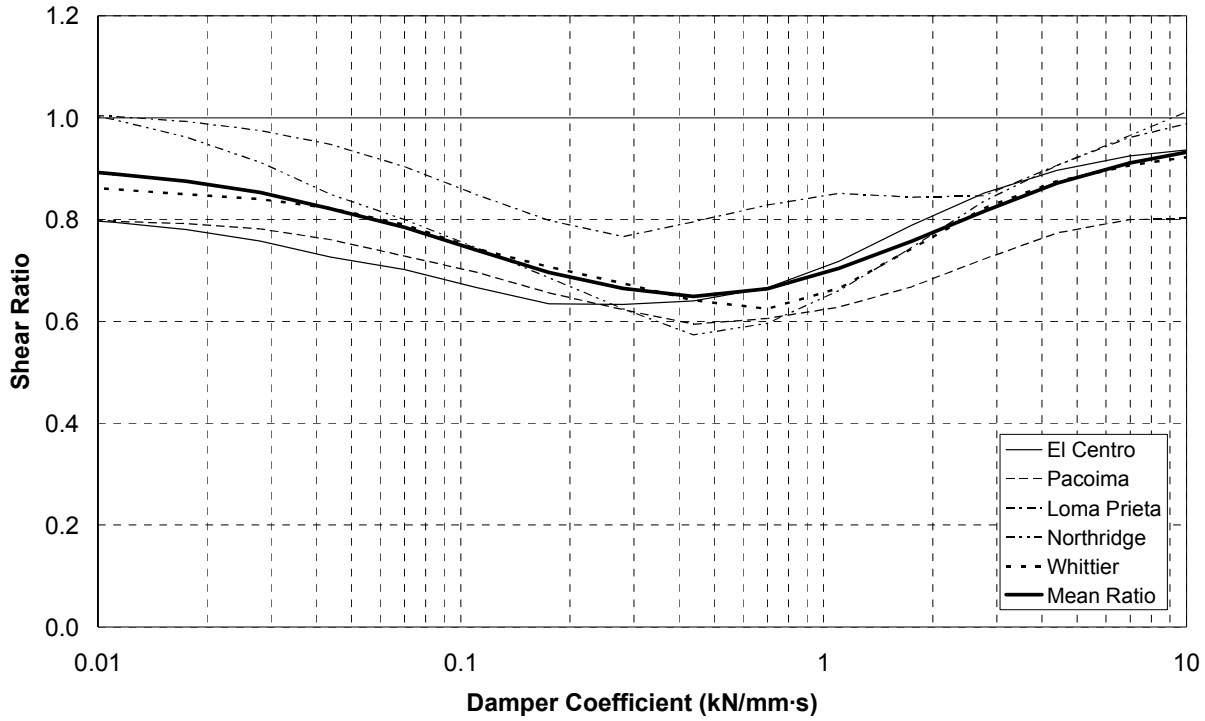

Figure 4.31 Shear connector stress ratio with VE dampers connected to abutments.

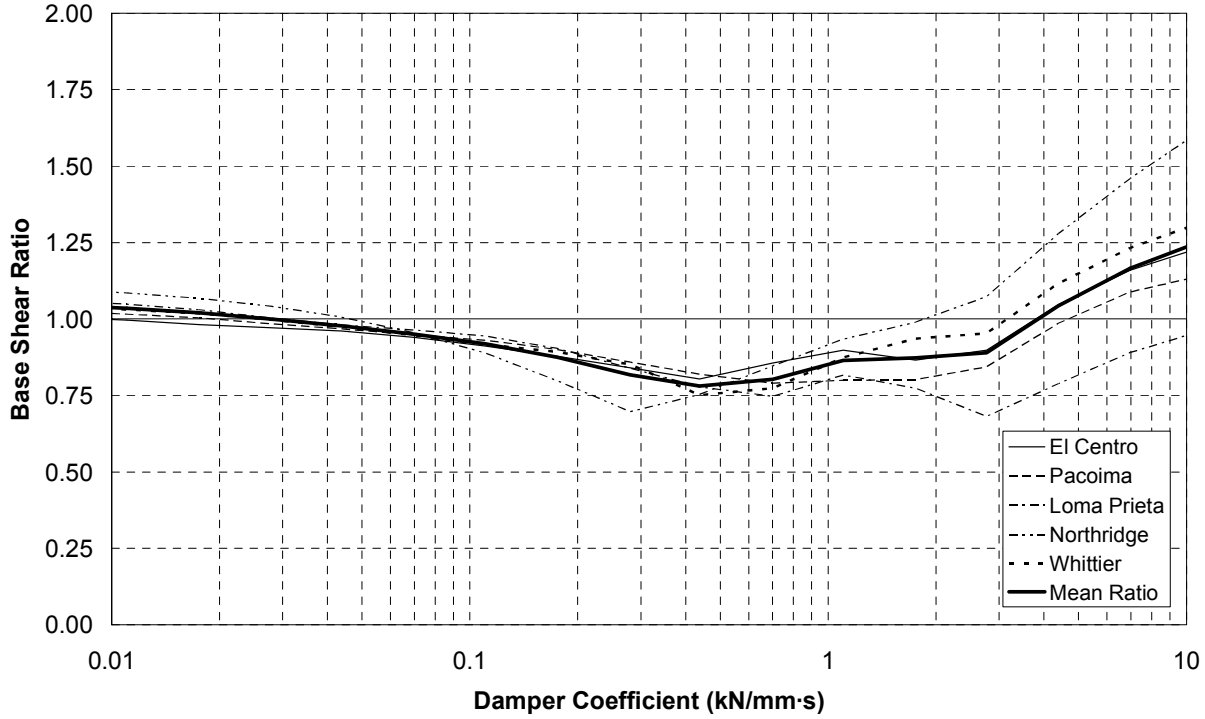

Figure 4.32 Base shear ratio with VE dampers connected to abutments.

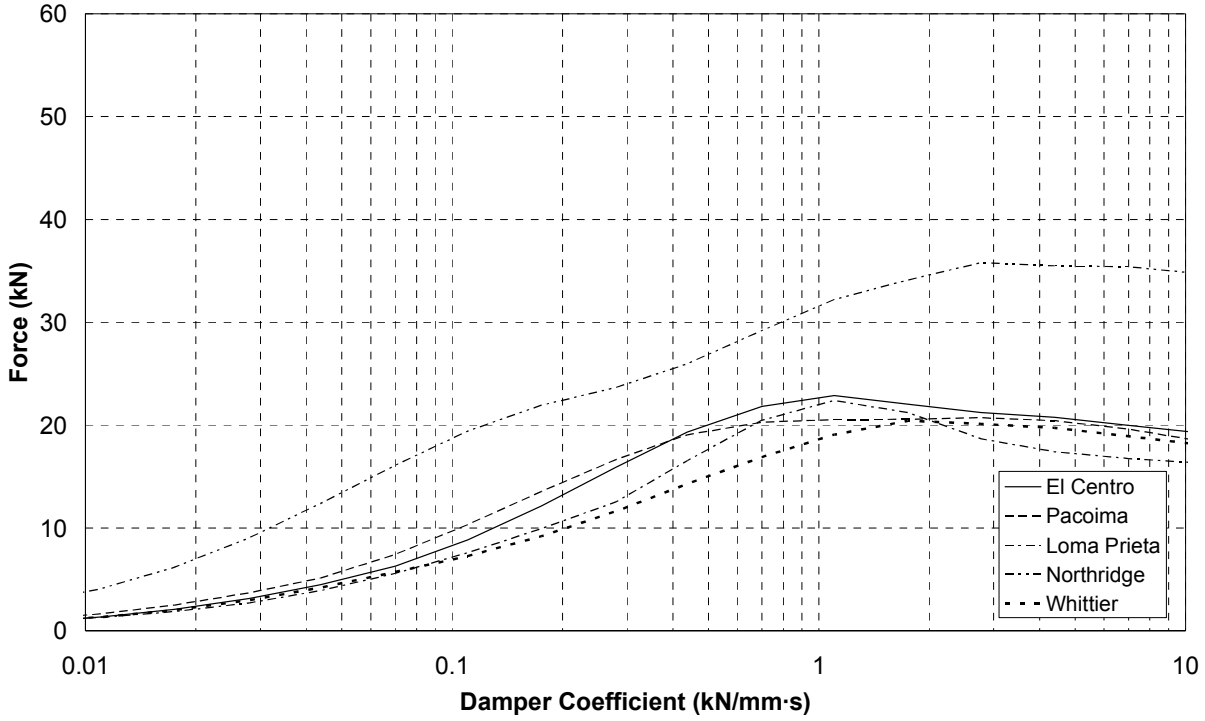

Figure 4.33 Peak damping forces in VE dampers connected to abutments.

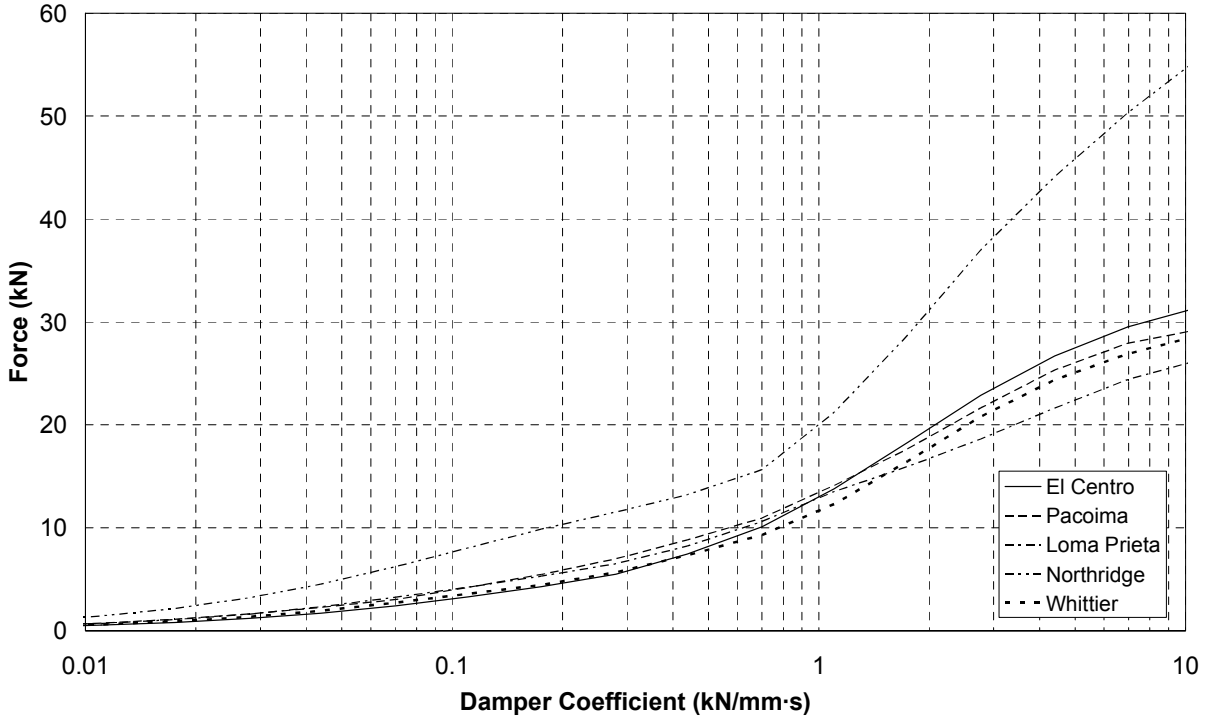

Figure 4.34 Peak stiffness forces in VE dampers connected to abutments.

4.4 Response with TADAS Elements

The TADAS elements were used in the same two brace configurations as the viscoelastic devices — the chevron braces and directly connected to the abutments. These devices performed acceptably in both configurations. They tended to perform slightly better than the friction dampers and viscoelastic dampers, but they did not perform as well as the viscous fluid dampers.

All of the TADAS elements were assumed to be constructed from mild steel. By varying the plate thickness, height, and base width, along with the number of plates used in a single device, both the elastic stiffness and the yield force could be adjusted independently over a wide range. For the model scale bridge, simulations were performed with TADAS elements having elastic stiffnesses from 11 kN/mm to 332 kN/mm, and with yield forces ranging from 9 kN to 90 kN. The upper end to the elastic stiffness was chosen because, even at the model scale, stiffer devices with the given range of yield forces were not physically practical.

The mean responses of the model scale bridge with TADAS elements in chevron braces, subjected to the five earthquake records, are shown in Figure 4.35 through Figure 4.38. The TADAS elements with the smallest elastic stiffnesses had little impact on the response of the bridge; however, as the device stiffness became larger, the devices with yield forces between 35 kN and 55 kN were able to reduce the deck displacements by more than 30% and the shear between the deck and the girders by more than 35%. These forces correspond to 45% to 70% of the tributary weight of the bridge.

The TADAS elements in this configuration had little impact on the shear forces between the superstructure and the abutments. The stiffest dampers reduced this response by only about four percent.

When the TADAS elements were connected directly to the bridge abutments, they further reduced the superstructure response at the expense of significantly increased base shears. As can be seen in Figure 4.39, the peak deck displacements were reduced by as much as 50%, while the peak shear forces between the deck and the girders, shown in Figure 4.40, were reduced by 40%.

Unfortunately, in this configuration the damper forces, shown in Figure 4.42, directly contributed to the forces transmitted to the abutments. As can be seen in Figure 4.41, these forces were always larger for the cases with the TADAS elements than for the bridge with a conventional diaphragm, and for the cases of the stiff dampers with large yield forces the base shears were greatly increased.

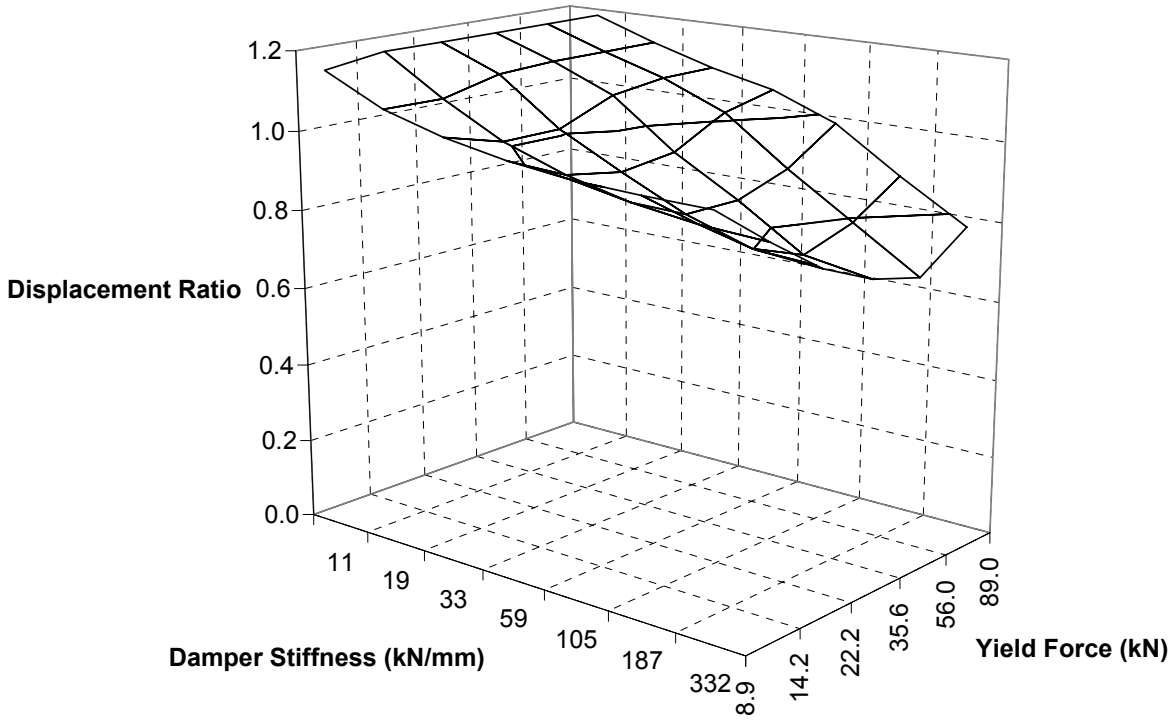

Figure 4.35 Deck displacement ratio with TADAS elements in chevron braces.

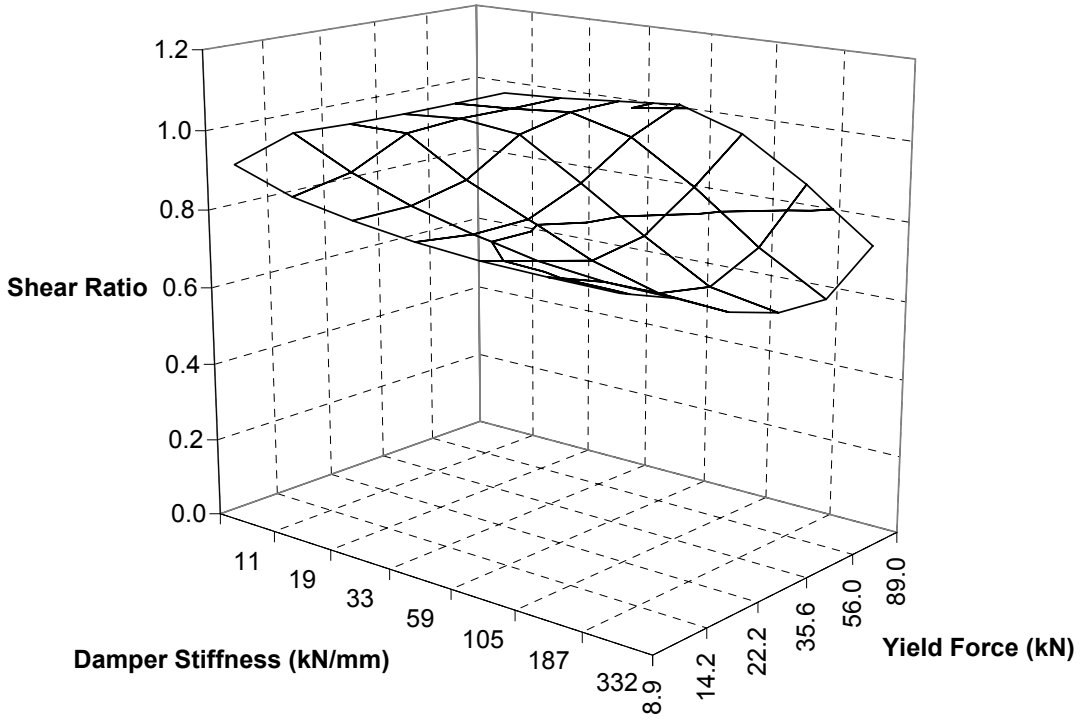

Figure 4.36 Shear connector stress ratio with TADAS elements in chevron braces.

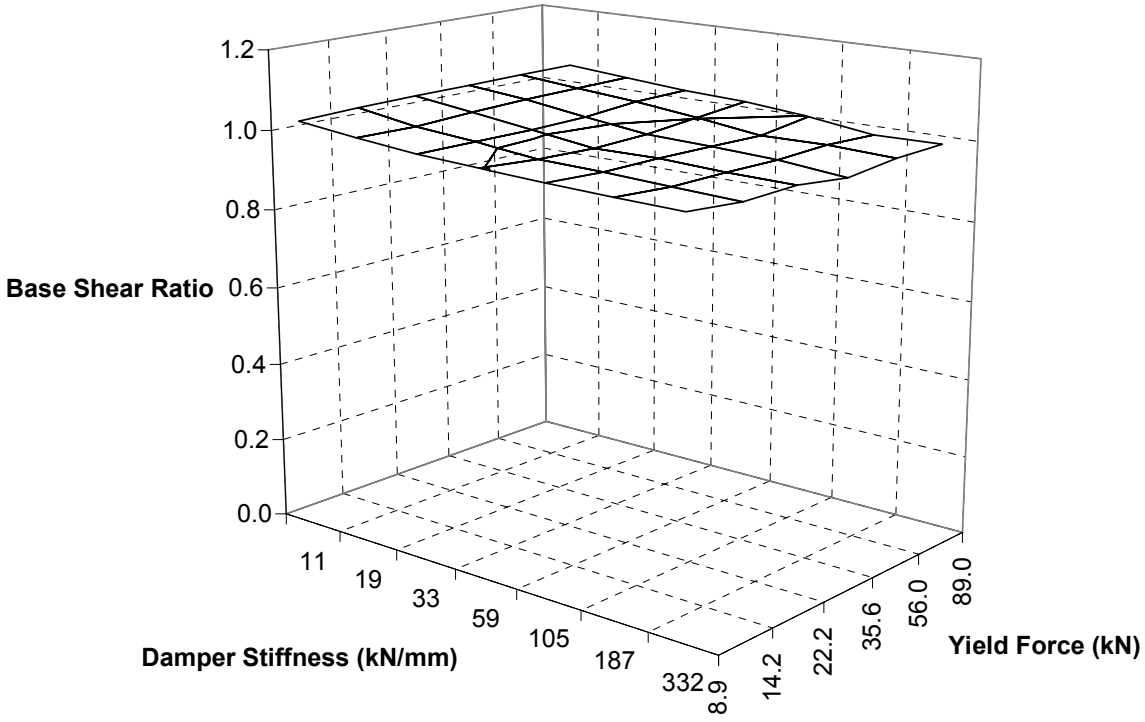

Figure 4.37 Base shear ratio with TADAS elements in chevron braces.

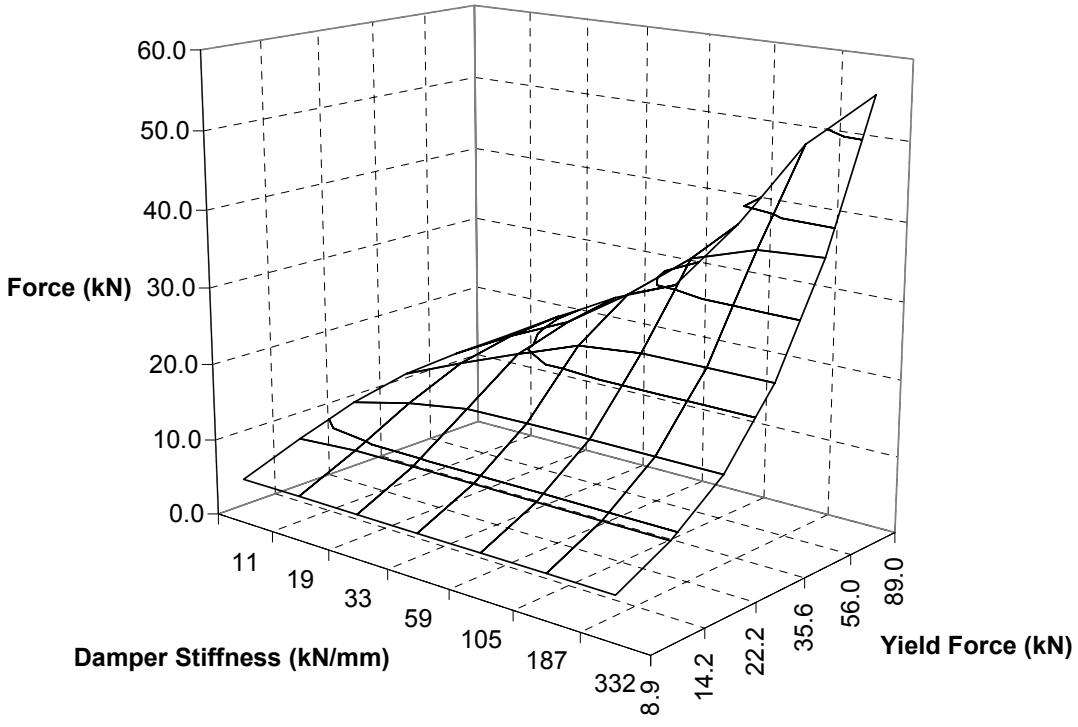

Figure 4.38 Peak forces in TADAS elements in chevron braces.

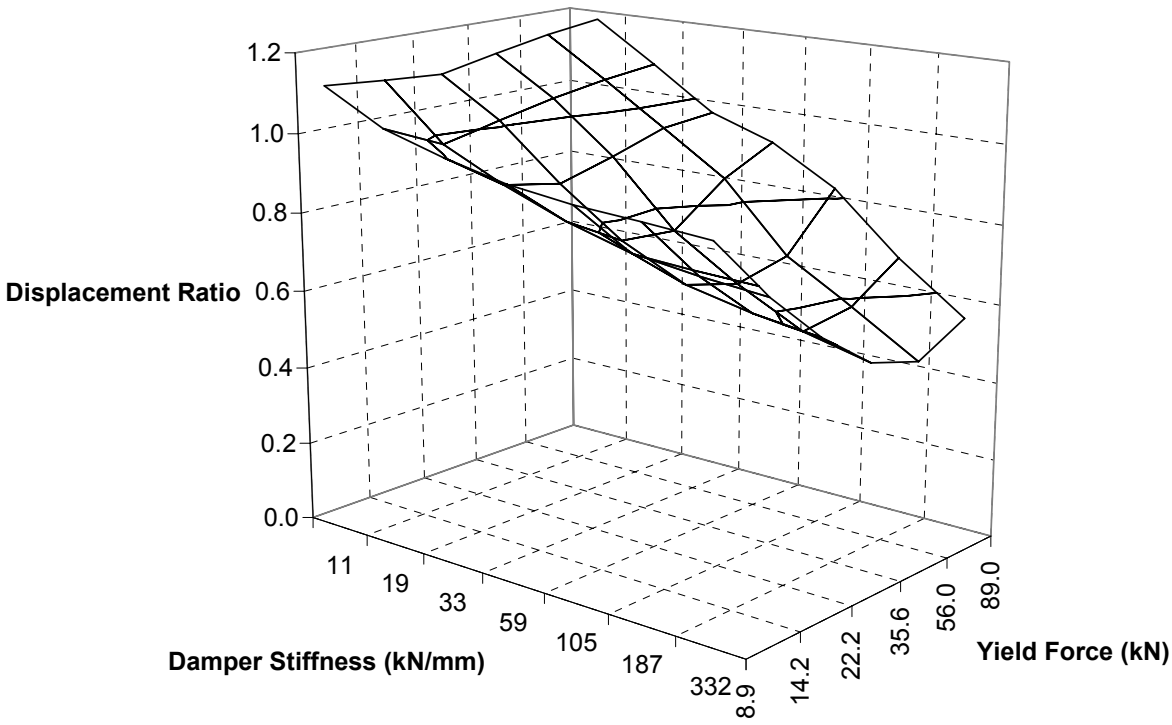

Figure 4.39 Deck displacement ratio with TADAS elements connected to abutments.

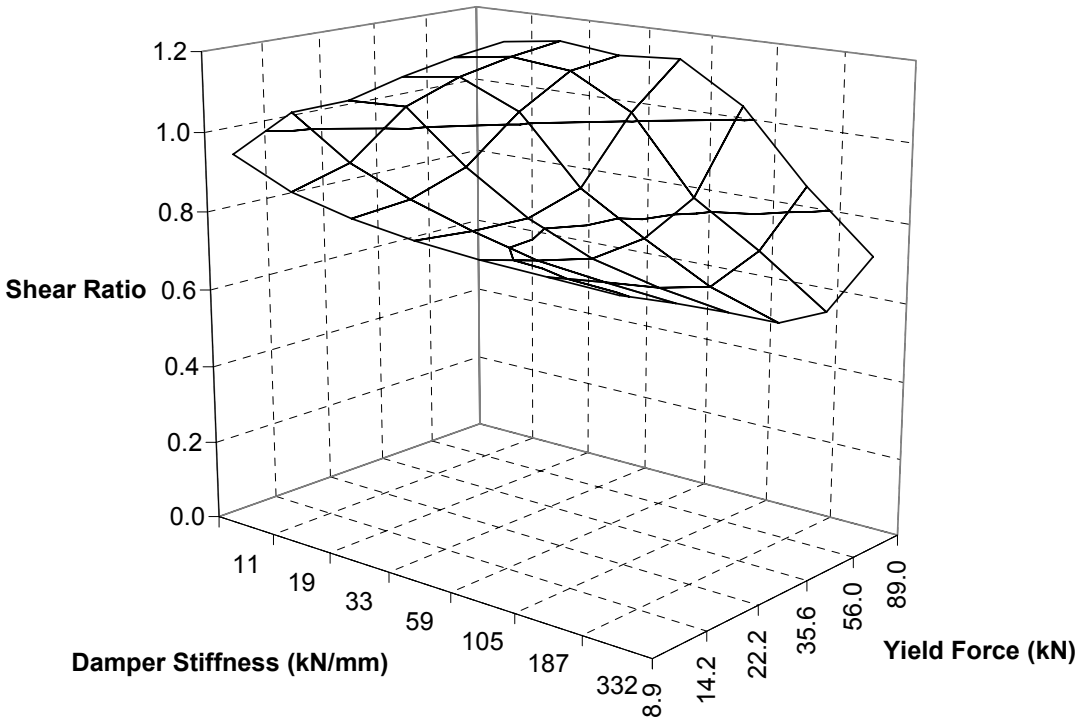

Figure 4.40 Shear connector stress ratio with TADAS elements connected to abutments.

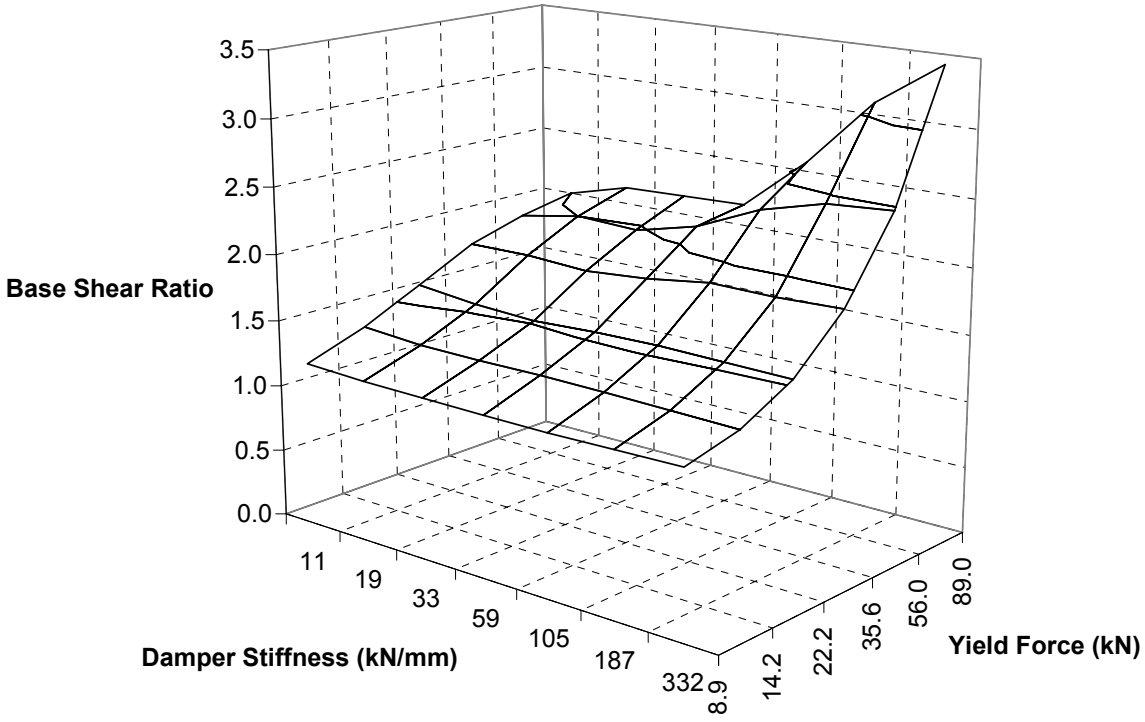

Figure 4.41 Base shear ratio with TADAS elements connected to abutments.

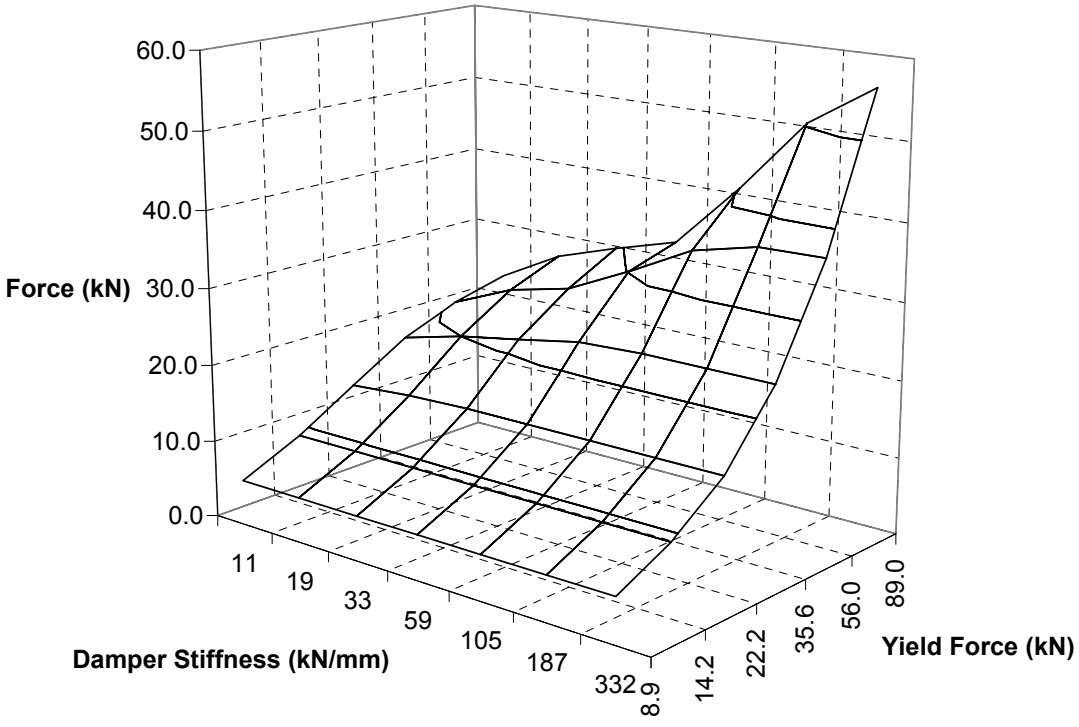

Figure 4.42 Peak forces in TADAS elements connected to abutments.

5 CONCLUSIONS

The results of the analyses summarized in this report show that energy dissipation devices located in ductile end diaphragms can significantly reduce the response of slab-on-girder bridges subjected to strong seismic excitation. All the devices and brace configurations that were considered were able to improve the response of the superstructure, although some devices and configurations were more effective than others. Unfortunately, only small reductions were obtained in the forces transmitted from the bridge to the substructure.

The viscous fluid dampers were able to greatly improve the response of the superstructure in all the brace configurations. These devices have the advantage of not having any inherent stiffness. When the dampers are properly sized for the application, the energy dissipation they provide more than compensates for the reduced stiffness. The latter tends to reduce the forces and stresses at the expense of the lateral displacements, and results in both reduced displacement response and reduced forces in the superstructure.

The friction dampers, viscoelastic dampers, and TADAS elements all improved the response of the superstructure when they were properly sized; however, the response improvements tended to be smaller than with the viscous fluid dampers. The choice of one of these devices for a particular application will be based more on cost and maintenance issues, as well as on temperature dependence, rather than on effectiveness alone.

Considering the cost and maintenance issues may change how the response results are interpreted. In particular, the viscous fluid dampers are potentially the most expensive of the devices considered in this report. Their superior response improvement makes them good candidates when potentially less expensive options cannot provide the necessary response reductions. The friction dampers and TADAS elements are relatively inexpensive by comparison, and may be preferable when lesser response reductions are necessary. Viscoelastic dampers are temperature sensitive, which when combined with their merely average response improvements, makes them an unlikely candidate for highway bridge applications.

All three brace configurations performed well, with no one configuration consistently performing better than the other two. The selection of a brace configuration is thus likely to be based on the practicality of using that configuration with the chosen energy dissipation system for a specific bridge.

The cross brace configuration, while simple in theory, may not always be practical in application. The lateral offset necessary to allow the braces to cross has the potential to create eccentric forces when used with large dampers, which can increase stresses at the connectors and may cause buckling of the struts.

The chevron brace configuration will generally be practical, but it may require significant strengthening of either the top or bottom struts in the diaphragm. The configuration that connects the dampers directly to the abutments has good potential for cases where the substructure has adequate reserve strength, but where the bearing strength is limited. Unfortunately, none of the configurations is appropriate when the substructure is inadequate for the seismic loads.

This page intentionally left blank.

6 REFERENCES

Astaneh-Asl, A., Bolt, B., McMullin, K., Modjtahedi, D., Cho, S., and Donikian, R. (1194). "Seismic performance of steel bridges during the 1994 Northridge Earthquake." *Report Number UCB/CE-Steel-94/01*, Dept. of Civil Engineering, University of California, Berkeley, Calif.

Hanson, R. D., and Soong, T. T. (2001). "Seismic Design with Supplemental Energy Dissipation Devices", *EERI Monograph MNO-8*, EERI, Oakland, CA.

Housner, G., and Thiel, C. (1995). "The continuing challenge: Report on the performance of state bridges in the Northridge Earthquake." *Earthquake Spectra*, 11(4), 607-636.

Sarraf, M. and Bruneau, M. (1998a). "Ductile Seismic Retrofit of Steel Deck-Truss Bridges. I: Strategy and Modeling", *Journal of Structural Engineering*, ASCE, 124(11), pp. 1253-1262.

Sarraf, M. and Bruneau, M. (1998b). "Ductile Seismic Retrofit of Steel Deck-Truss Bridges. II: Design Applications", *Journal of Structural Engineering*, ASCE, 124(11), pp. 1263-1271.

Soong, T. T., and Dargush, G. F. (1997). *Passive Energy Dissipation Systems in Structural Engineering*, John Wiley& Sons, New York, NY.

Tsai, K. C., Chen, H. W., Hong, C. P., and Su, F. Y. (1993). "Design of Steel Triangular Plate Energy Absorbers for Seismic-resistant Construction", *Earthquake Spectra*, 9(3), 505-528.

Zahrai, S. M. and Bruneau, M. (1998). "Impact of Diaphragms on the Seismic Response of Straight Slab-On-Girder Steel Bridges", *Journal of Structural Engineering*, ASCE, 124(8), pp. 938-947.

Zahrai, S. M. and Bruneau, M. (1999a). "Ductile End Diaphragms for Seismic Retrofit of Slab-On-Girder Steel Bridges", *Journal of Structural Engineering*, ASCE, 125(1), pp. 71-80.

Zahrai, S. M. and Bruneau, M. (1999b). "Cyclic Testing of Ductile End Diaphragms for Slab-On-Girder Steel Bridges", *Journal of Structural Engineering*, ASCE, 125(9), pp. 987-996.